PREPRINT 440

DECEMBER 2015

A new hydrostatic reconstruction scheme motivated by the wet-dry front

Guoxian Chen* and Sebastian Noelle†

Institut für Geometrie und Praktische Mathematik
Templergraben 55, 52062 Aachen, Germany

* School of Mathematics and Statistics, Wuhan University, Wuhan, 430072, P.R. China.
† IGPM, RWTH Aachen University, Templergraben 55, 52062, Aachen, Germany.
Email addresses: gxchen.math@whu.edu.cn, noelle@igpm.rwth-aachen.de

A new hydrostatic reconstruction scheme motivated by the wet-dry front

Guoxian Chen [*] Sebastian Noelle [†]

December 11, 2015

Abstract

A key difficulty in the analysis and numerical approximation of the shallow water equations is the non-conservative product of measures due to the gravitational force acting on a sloped bottom. Solutions may be non-unique, and numerical schemes are not only consistent discretizations of the shallow water equations, but they also make a decision how to model the physics. Our derivation is based on infinitesimal singular layers at the cell boundaries, as inspired by [Noelle, Xing, Shu, JCP 2007]. One key step is to separate the singular measures. Another aspect is the reconstruction of the solution variables in the singular layers. We study three reconstructions. The first leads to the well-known scheme of [Audusse, Bristeau, Bouchut, Klein, Perthame, SISC 2004], which introduces the hydrostatic reconstruction. The second is a modification proposed in [Morales, Castro, Pares, AMC 2013], which analyzes if a wave has enough energy to overcome a step. The third is our new scheme, and borrows its structure from the wet-dry front. For a number of cases discussed in recent years, where water runs down a hill, Audusse' scheme converges slowly or fails. Morales' scheme gives a visible improvement. Both schemes are clearly outperformed by our new scheme.

Keywords: Shallow water equations, water at rest, well balanced property, wet-dry front, nonconservative products of measures.

AMS subject classifications. 76M12, 35L65,

1 Introduction

In this paper, we consider a class of finite volume schemes for the shallow water equations with variable bottom topography. These equations are a prototype of hyperbolic balance laws.

Balance laws often consist of the conservation laws for the vector $U(x,t)$ of mass and momentum, accelerated by conservative advection and pressure forces (denoted by $-\partial F(U)/\partial x$ in (1.1) below), and by additional non-conservative forces $S(U,x)$, also called source terms. Hence the equations of motion may be written as

$$\frac{\partial U}{\partial t}+\frac{\partial F(U)}{\partial x}=S(U,x). \tag{1.1}$$

[*]School of Mathematics and Statistics, Wuhan University, Wuhan, 430072, P.R. China.
[†]IGPM, RWTH Aachen University, Templergraben 55, 52062, Aachen, Germany.
Email addresses: gxchen.math@whu.edu.cn, noelle@igpm.rwth-aachen.de

In this paper, there is no source term in the equation of mass, so we can write $S=(0,s)^T$.

A particular challenge is the analytical and numerical understanding of near-equilibrium flows, for which the residuum

$$R(x,t) := -\frac{\partial F(U)}{\partial x} + S(U,x) \tag{1.2}$$

nearly vanishes.

A semi-discrete, first order accurate finite volume scheme may be written as a method of lines,

$$\frac{d}{dt} U_i(t) = R_i(t) \tag{1.3}$$

where $U_i(t)$ approximates the cell average over cell $C_i = [x_{i-\frac{1}{2}}, x_{i+\frac{1}{2}}]$ at time t, and $R_i(t)$ is the cell average of the residuum, given by

$$R_i(t) := -\frac{1}{\Delta x}\left(F_{i+\frac{1}{2}} - F_{i-\frac{1}{2}}\right) + S_i. \tag{1.4}$$

Here $\Delta x = x_{i+\frac{1}{2}} - x_{i-\frac{1}{2}}$ is the spatial grid size, $F_{i\pm 1/2}$ is a conservative numerical flux function, and S_i approximates the cell average of the source term. Lax and Wendroff proved in 1960 that limits of conservative numerical schemes are weak solutions of the corresponding systems of hyperbolic conservation laws [Lax and Wendroff, 1960]. There are many well-established conservative numerical fluxes (usually called approximate Riemann solvers), see e.g. [Roe, 1981, Harten et al., 1983, Godlewski and Raviart, 1996, Toro, 1999, Bouchut, 2004] and the references therein. On the other hand, there is no general procedure to discretize the source term.

Indeed, it is a challenge for each balance law, each equilibrium state, and each numerical flux function to find a discretization of the source which preserves desirable stability properties. There is, however, one common feature to most balance laws: since the force in Newton's law equals mass times acceleration, the source term $S(U,x)$ is often a product term. Each of the factors may become a singular measure at the cell boundaries, and sometimes their product cannot be evaluated. In [Dal Maso et al., 1995], DalMaso, LeFloch and Murat present a theory of nonconservative products of measures. This was systematically extended to a numerical framework of path-conservative schemes by Pares, Castro et al. (see [Parés, 2006, Castro et al., 2006]). However, the limits of these schemes are not unique, and any choice of path implies a - perhaps tacit - modelling assumption (see the discussion in [Castro et al., 2008, Abgrall and Karni, 2010, Muñoz-Ruiz and Parés, 2011]).

In this work, we focus on the one-dimensional shallow water equations, given by

$$U = \begin{pmatrix} h \\ hu \end{pmatrix}, \quad F(U) = \begin{pmatrix} hu \\ hu^2 + \frac{1}{2}gh^2 \end{pmatrix} \quad \text{and} \quad S(U,x) = -\begin{pmatrix} 0 \\ ghz_x \end{pmatrix}. \tag{1.5}$$

Here $z(x)$ is the bottom topography, $h(x,t)$ the water depth, $u(x,t)$ the water velocity, and $g = 9.8\text{m/s}^2$ the gravitational acceleration. Thus the source term models the force of gravity tangential to a sloped bottom. It is instructive to rewrite the residuum as

$$R = \begin{pmatrix} hu \\ hu^2 \end{pmatrix}_x + gh \begin{pmatrix} 0 \\ w \end{pmatrix}_x, \tag{1.6}$$

where $w = z + h$ is the water level. Two important equilibria are

(i) *still water*, where

$$u = 0 \quad \text{and} \quad w_x = 0$$

(ii) the *lake at rest*, which is still water together with dry boundaries:

$$u = 0 \quad \text{and} \quad hw_x = 0.$$

Hence the lake at rest residuum combines the dry shore $(h = 0)$ with the flat water level $(w_x = 0)$ in a single product. We will use this elegant expression subsequently to split the non-conservative product of measures. This will yield the new hydrostatic reconstruction scheme.

The paper is organized as follows: In Section 2, we summarize two known, i.e. the original one introduced in [Audusse et al., 2004] and its modification by [Morales de Luna et al., 2013], and a new hydrostatic reconstruction (HR) scheme. In Section 3 we re-derive the three HR methods by an infinitesimal limit process. The advantage of this process will be that it gives an explicit treatment of the non-conservative product. It consist of four steps: (1) splitting the cells into subcells; (2) reconstruction of the bottom; (3) infinitesimal hydrostatic reconstruction; (4) fluxes and source terms based on subcell reconstructions. In Section 4, we establish the stability of the new HR scheme: positivity of the water height; well-balanced property for the lake at rest; and a semi-discrete entropy inequality. Finally in Section 5, several numerical experiments allow to compare the three HR schemes.

2 Definition of the hydrostatic reconstruction schemes

In this section, we summarize two known and a new hydrostatic reconstruction scheme. Each of them introduces reconstructed values $U_{i+\frac{1}{2}\pm}$ of the unknowns to the left and right of interface $x_{i+\frac{1}{2}}$, and defines the numerical flux via a Riemann solver $\mathcal{F}$,

$$F_{i+\frac{1}{2}} = \mathcal{F}(U_{i+\frac{1}{2}-}, U_{i+\frac{1}{2}+}).$$

Then the schemes split the singular source term at the interface into a left and a right part, $S_{i+\frac{1}{2}-}$ and $S_{i+\frac{1}{2}+}$ and compute the source term in (1.4) as

$$S_i = S_{i-\frac{1}{2}+} + S_{i+\frac{1}{2}-} = \left(0, s_{i-\frac{1}{2}+}\right)^T + \left(0, s_{i+\frac{1}{2}-}\right)^T. \tag{2.1}$$

A key ingredient of this splitting is the definition of an intermediate bottom level $z_{i+\frac{1}{2}}$ at the interface.

There will be two main types of interface, depending on how the water covers the bottom to the left and right side of the interface (see Figure 1. First, there is the *fully wet interface*, where the water level on each side is higher than the higher side of the bottom topograpy,

$$\min(w_i, w_{i+1}) > \max(z_i, z_{i+1}). \tag{2.2}$$

Second, there is the *partially wet interface*, where the water level on one side is equal or below the topography on the other side,

$$\min(w_i, w_{i+1}) \leq \max(z_i, z_{i+1}). \tag{2.3}$$

The partially wet case includes subcases where one or both of the cells adjacent to the interface contain no water. In this case we call the interface partially dry, or dry.

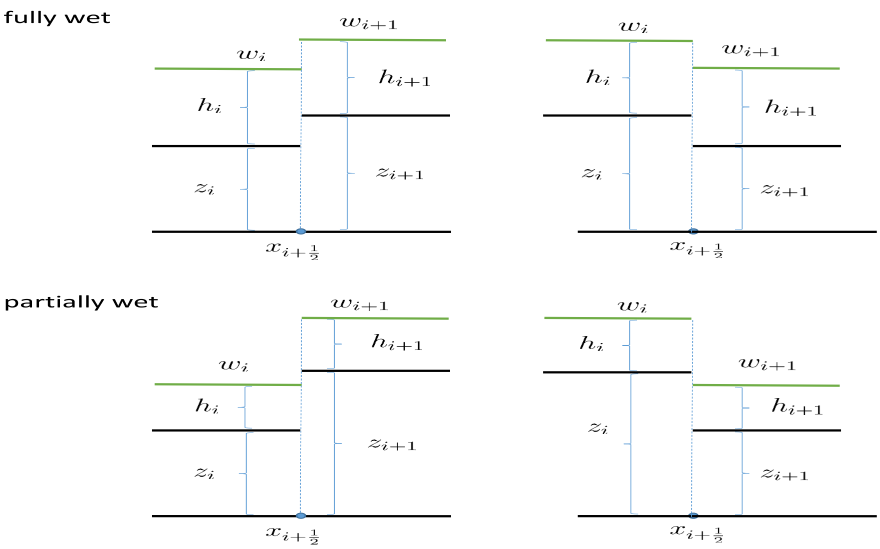

Figure 1: Examples of interfaces: fully wet (top), and partially wet (bottom).

In the following, we distinguish the three HR schemes by superscripts such as $h^{\mathrm{AUD}}_{i+\frac{1}{2}\pm}$, $h^{\mathrm{MOR}}_{i+\frac{1}{2}\pm}$, and $h^{\mathrm{CN}}_{i+\frac{1}{2}\pm}$ for the schemes of Audusse' et al., the modification due to Morales et al., and the present scheme, respectively. After the water heights $h_{i-\frac{1}{2}+}$ and $h_{i+\frac{1}{2}-}$ are reconstructed, we define the conservative variables as

$$U_{i+\frac{1}{2}-} = h_{i+\frac{1}{2}-} u_i, \qquad U_{i-\frac{1}{2}+} = h_{i-\frac{1}{2}+} u_i. \tag{2.4}$$

Before we give a derivation of the method in terms of singular layers (see Section 3), we first introduce the three HR schemes.

2.1 The original HR method

Audusse et al. [Audusse et al., 2004] introduced their first order hydrostatic reconstruction scheme by choosing the intermediate bottom as

$$z^{\mathrm{AUD}}_{i+\frac{1}{2}} := \max(z_i, z_{i+1}), \tag{2.5}$$

the interface water heights as

$$h^{\mathrm{AUD}}_{i-\frac{1}{2}+} := \max(w_i - z^{\mathrm{AUD}}_{i-\frac{1}{2}}, 0), \quad h^{\mathrm{AUD}}_{i+\frac{1}{2}-} := \max(w_i - z^{\mathrm{AUD}}_{i+\frac{1}{2}}, 0) \tag{2.6}$$

Then they discretize the source term as

$$s^{\mathrm{AUD}}_{i-\frac{1}{2}+} := \frac{g}{2\Delta x}\big((h_i)^2 - (h^{\mathrm{AUD}}_{i-\frac{1}{2}+})^2\big), \tag{2.7}$$

$$s^{\mathrm{AUD}}_{i+\frac{1}{2}-} := \frac{g}{2\Delta x}\big((h^{\mathrm{AUD}}_{i+\frac{1}{2}-})^2 - (h_i)^2\big). \tag{2.8}$$

2.2 The HR method of Morales et. al.

The hydrostatic reconstruction scheme of Morales et al. [Morales de Luna et al., 2013] is identical with that of Audusse's scheme,

$$z^{\mathrm{MOR}}_{i+\frac{1}{2}} := z^{\mathrm{AUD}}_{i+\frac{1}{2}}, \quad h^{\mathrm{MOR}}_{i+\frac{1}{2}-} := h^{\mathrm{AUD}}_{i+\frac{1}{2}-}, \quad h^{\mathrm{MOR}}_{i+\frac{1}{2}+} := h^{\mathrm{AUD}}_{i+\frac{1}{2}+}, \tag{2.9}$$

and the source term is defined as

$$s^{\mathrm{MOR}}_{i+\frac{1}{2}-} := s^{\mathrm{AUD}}_{i+\frac{1}{2}-}, \quad s^{\mathrm{MOR}}_{i+\frac{1}{2}+} := s^{\mathrm{AUD}}_{i+\frac{1}{2}+}, \tag{2.10}$$

except for the partially wet interfaces (2.3), where water either flows downhill, or it flows uphill with enough kinetic energy to climb the jump of the bottom at the interface. This results in the following two cases:

(i) (*ascending bottom*) $z_i < z_{i+1}$. If $u_i < 0$, or $u_i > 0$ and

$$\frac{|u_i|^2}{2} + g(w_i - z_{i+1}) \geq \frac{3}{2}\sqrt{g(h_i|u_i|)^3}. \tag{2.11}$$

then the left interface source term is redefined as

$$s^{\mathrm{MOR}}_{i+\frac{1}{2}-} := -\frac{g}{\Delta x}\frac{h_i}{2}\left(z^{\mathrm{MOR}}_{i+\frac{1}{2}} - z_i\right). \tag{2.12}$$

(ii)(*descending bottom*) $z_i > z_{i+1}$. If $u_{i+1} > 0$, or $u_{i+1} < 0$ and

$$\frac{|u_{i+1}|^2}{2} + g(w_{i+1} - z_i) \geq \frac{3}{2}\sqrt{g(h_{i+1}|u_{i+1}|)^3}, \tag{2.13}$$

then the right interface source term is redefined as

$$s^{\mathrm{MOR}}_{i+\frac{1}{2}+} := -\frac{g}{\Delta x}\frac{h_{i+1}}{2}\left(z_{i+1} - z^{\mathrm{MOR}}_{i+\frac{1}{2}}\right). \tag{2.14}$$

2.3 The present HR method

For the present HR method the intermediate bottom is defined as

$$z^{\mathrm{CN}}_{i+\frac{1}{2}} := \min\left(\max(z_i, z_{i+1}), \min(w_i, w_{i+1})\right). \tag{2.15}$$

The interface water heights are given by

$$h^{\mathrm{CN}}_{i+\frac{1}{2}-} := \min(w_i - z^{\mathrm{CN}}_{i+\frac{1}{2}}, h_i), \quad h^{\mathrm{CN}}_{i+\frac{1}{2}+} := \min(w_{i+1} - z^{\mathrm{CN}}_{i+\frac{1}{2}}, h_{i+1}), \tag{2.16}$$

and the interface source terms are defined as

$$s^{\mathrm{CN}}_{i+\frac{1}{2}-} := -\frac{g}{\Delta x}\frac{h_i + h^{\mathrm{CN}}_{i+\frac{1}{2}-}}{2}\left(z^{\mathrm{CN}}_{i+\frac{1}{2}} - z_i\right). \tag{2.17}$$

$$s^{\mathrm{CN}}_{i+\frac{1}{2}+} := -\frac{g}{\Delta x}\frac{h^{\mathrm{CN}}_{i+\frac{1}{2}+} + h_{i+1}}{2}\left(z_{i+1} - z^{\mathrm{CN}}_{i+\frac{1}{2}}\right). \tag{2.18}$$

3 Interpretation via subcell reconstructions

In (1.3)–(1.4), we introduced the semi-discrete finite volume scheme as

$$\frac{d}{dt}U_i(t) = R_i = -\frac{1}{\Delta x}\left(F_{i+\frac{1}{2}} - F_{i-\frac{1}{2}}\right) + S_i. \tag{3.1}$$

We reviewed three hydrostatic reconstruction schemes which fit into this framework and discussed the difficulty of nonconservative products in the singular source terms at the cell interfaces.

In the present section, we rederive schemes of the form (3.1) by an infinitesimal limit process. The advantage of this process will be that it gives an explicit treatment of the non-conservative product.

We begin by replacing the interfaces $x_{i+\frac{1}{2}}$ by singular layers (or internal boundary layers)

$$\widehat{C}^{\varepsilon}_{i+\frac{1}{2}} := [x_{i+\frac{1}{2}} - \varepsilon, x_{i+\frac{1}{2}} + \varepsilon].$$

Over each of these infinitesimal layers the bottom is reconstructed continuously by a function $z_\varepsilon(x)$. This removes the non-conservative product. The flow variables are reconstructed by piecewise continuous functions $h_\varepsilon(x)$, $w_\varepsilon(x)$, and $u_\varepsilon(x)$ over the singular subcells

$$\widehat{C}^{\varepsilon}_{i+\frac{1}{2}-} := [x_{i+\frac{1}{2}} - \varepsilon, x_{i+\frac{1}{2}}] \quad \text{and} \quad \widehat{C}^{\varepsilon}_{i+\frac{1}{2}+} := [x_{i+\frac{1}{2}}, x_{i+\frac{1}{2}} + \varepsilon].$$

These reconstructions provide the data of the Riemann problem at the interface, with an approximate Riemann solver $F_\varepsilon(x_{i+\frac{1}{2}})$. The source term is computed over the singular subcells. Together, this gives the residuum

$$R_i^\varepsilon := -\frac{1}{\Delta x}\left(F_\varepsilon(x_{i+\frac{1}{2}}) - F_\varepsilon(x_{i-\frac{1}{2}})\right) + \frac{1}{\Delta x}\int\limits_{C_i} S(U_\varepsilon(x), z_\varepsilon(x))dx. \tag{3.2}$$

In Theorem 3.5 we prove that

$$\lim_{\varepsilon\to 0} R_i^\varepsilon = R_i, \tag{3.3}$$

where R_i is the original residuum from (3.1).

Remark 3.1. *(i) Note that the construction procedure summarized in (3.3) has already been used in [Noelle et al., 2007, Noelle et al., 2009] to define a high-order well-balanced scheme for moving water. Here we use it to derive a new hydrostatic reconstruction scheme, which is tailored to the wet-dry front.*
(ii) In Remark 3.6 below, we will use the subcell reconstruction to highlight a key difference between the three schemes.
(iii) It is an interesting question under which conditions a subcell reconstruction may be interpreted as a path in the sense of [Dal Maso et al., 1995, Parés, 2006].

The details of the approximation are given in the following subsections.

3.1 Splitting the cells into subcells

Let us denote the interior subcell by $C_i^\varepsilon := \left[x_{i-\frac{1}{2}} + \varepsilon, x_{i+\frac{1}{2}} - \varepsilon\right]$. Then

$$C_i = \widehat{C}^{\varepsilon}_{i-\frac{1}{2}+} \cup C_i^\varepsilon \cup \widehat{C}^{\varepsilon}_{i+\frac{1}{2}-}. \tag{3.4}$$

The piecewise continuous reconstruction is defined as follows:

Definition 3.2. (subcell reconstruction) *Let* $\varphi_\varepsilon : \mathbf{R} \to \mathbf{R}$ *be Lipschitz-continuous over each cell* C_i *with possible discontinuities at the interfaces* $x_{i+\frac{1}{2}}$. *Given values*

$$\varphi_{i-\frac{1}{2}+}, \quad \varphi_i, \quad \varphi_{i+\frac{1}{2}-}, \tag{3.5}$$

let

$$\varphi_\varepsilon(x) := \begin{cases} \widehat{\varphi}^\varepsilon_{i-\frac{1}{2}+}(x) & \textit{if } x \in \widehat{C}^\varepsilon_{i-\frac{1}{2}+}, \\ \varphi_i & \textit{if } x \in C^\varepsilon_i, \\ \widehat{\varphi}^\varepsilon_{i+\frac{1}{2}-}(x) & \textit{if } x \in \widehat{C}^\varepsilon_{i+\frac{1}{2}-} \end{cases} \tag{3.6}$$

where $\widehat{\varphi}^\varepsilon_{i-\frac{1}{2}+}(x_{i-\frac{1}{2}}) = \varphi_{i-\frac{1}{2}+}$ *and* $\widehat{\varphi}^\varepsilon_{i+\frac{1}{2}-}(x_{i+\frac{1}{2}}) = \varphi_{i+\frac{1}{2}-}$.

Remark 3.3. *(i) While Definition 3.2 is formulated over each cell, we are really interested in the the pair of subcell reconstructions* $\widehat{\varphi}^\varepsilon_{i+\frac{1}{2}-} : \widehat{C}^\varepsilon_{i+\frac{1}{2}-} \to \mathbf{R}$ *and* $\widehat{\varphi}^\varepsilon_{i+\frac{1}{2}+} : \widehat{C}^\varepsilon_{i+\frac{1}{2}+} \to \mathbf{R}$ *at an interface* $x_{i+\frac{1}{2}}$.

(ii) If $\widehat{\varphi}^\varepsilon_{i+\frac{1}{2}-}$ *and* $\widehat{\varphi}^\varepsilon$ *are both linear, we call them the* standard subcell reconstruction at interface $x_{i+\frac{1}{2}}$.

(iii) The only exception from the standard subcell reconstruction will occur in the definition of the water level for Audusse' and Morales' scheme for partially wet interfaces (see equations (3.15) – (3.16) *and Figure 3 below).*

To distinguish the related reconstructions for the three HR schemes of Audusse, Morales, and the present paper, we will denote them by

$$\varphi^{\mathrm{AUD}}_\varepsilon, \varphi^{\mathrm{MOR}}_\varepsilon, \varphi^{\mathrm{CN}}_\varepsilon. \tag{3.7}$$

3.2 Reconstruction of the bottom $z_\varepsilon(x)$

For all three HR schemes, a continuous bottom is defined by the standard subcell reconstruction (see Definition 3.2) with

$$z_{i-\frac{1}{2}+} := z_{i-\frac{1}{2}}, \quad z_{i+\frac{1}{2}-} := z_{i+\frac{1}{2}}, \tag{3.8}$$

where the values $z_{i\pm\frac{1}{2}}$ are defined in Section 2 for each of the three schemes, respectively.

Note that the reconstructed bottom is globally continuous for fixed $\varepsilon > 0$, but will have steep layers in $\hat{C}^\varepsilon_{i+\frac{1}{2}-}$ and $\hat{C}^\varepsilon_{i+\frac{1}{2}+}$.

3.3 Infinitesimal hydrostatic reconstruction

Next we reconstruct the water level and height. Several modern well-balanced schemes such as [Zhou et al., 2001, Kurganov and Levy, 2002], as well as the present hydrostatic reconstruction schemes use the fact that the water level $w(x)$ is constant for still water. Hence the piecewise constant reconstruction becomes exact for this important equilibrium state. Given the bottom topography $z_\varepsilon(x)$, these schemes reconstruct the water level $w_\varepsilon(x)$ and then simply define the reconstructed water height as

$$h_\varepsilon(x) = w_\varepsilon(x) - z_\varepsilon(x). \tag{3.9}$$

The conservative variables are given by

$$U_\varepsilon(x) = \begin{pmatrix} h_\varepsilon(x) \\ h_\varepsilon(x)u_i \end{pmatrix} \qquad \forall x \in C_i. \tag{3.10}$$

3.3.1 The original HR method

We define $w_\varepsilon(x)$ as in Definition 3.2, with

$$w_i^{\text{AUD}} := z_i + h_i, \quad w_{i+1}^{\text{AUD}} := z_{i+1} + h_{i+1}, \tag{3.11}$$

$$w_{i+\frac{1}{2}-}^{\text{AUD}} := \max(z_{i+\frac{1}{2}}^{\text{AUD}}, w_i), \quad w_{i+\frac{1}{2}+}^{\text{AUD}} := \max(z_{i+\frac{1}{2}}^{\text{AUD}}, w_{i+1}). \tag{3.12}$$

In the fully wet case (see Figure 2),

$$\widehat{w}_{i+\frac{1}{2}-}^{\text{AUD}}(x) \equiv w_i, \tag{3.13}$$

$$\widehat{w}_{i+\frac{1}{2}+}^{\text{AUD}}(x) \equiv w_{i+1}, \tag{3.14}$$

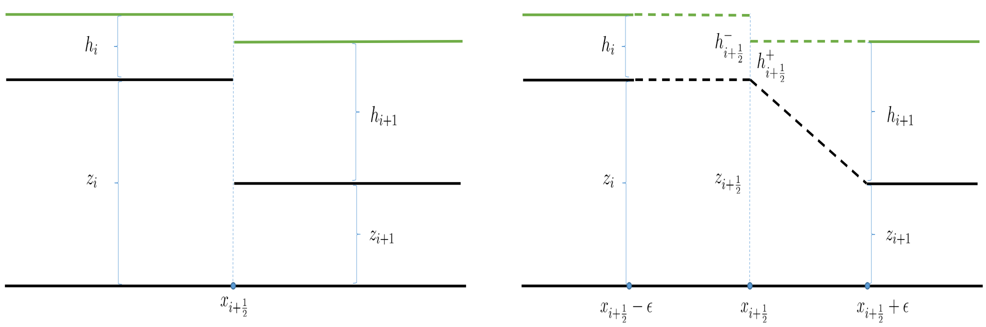

Figure 2: Subcell reconstruction of the water level in the fully wet case. left: Jump data; right: Reconstructed $w_\varepsilon(x)$.

while in the partially wet case (see Figure 3),

$$\widehat{w}_{i+\frac{1}{2}-}^{\text{AUD}}(x) := \max(z_\varepsilon^{\text{AUD}}(x), w_i), \tag{3.15}$$

$$\widehat{w}_{i+\frac{1}{2}+}^{\text{AUD}}(x) := \max(z_\varepsilon^{\text{AUD}}(x), w_{i+1}). \tag{3.16}$$

This is the only instance where our subcell reconstruction may differ from the standard definition. In fact, this will happen if and only if the wet-dry front is contained in one of the cells $\widehat{C}^\varepsilon_{i+\frac{1}{2}-}$ or $\widehat{C}^\varepsilon_{i+\frac{1}{2}+}$ (compare Figure 3).

Next, we consider the average of $h_\varepsilon^{\text{AUD}}(x)$ over subcells $\widehat{C}^\varepsilon_{i+\frac{1}{2}-}$ and $\widehat{C}^\varepsilon_{i+\frac{1}{2}+}$. We first consider $\widehat{C}^\varepsilon_{i+\frac{1}{2}+}$. There are two cases to be discussed:

(i) In the fully wet case (in which all three schemes coincide) the water height $\widehat{h}^{\text{AUD}}_{i+\frac{1}{2}+}$ is linear, so

$$\overline{h}^{\text{AUD}}_{i+\frac{1}{2}+} = \frac{h^{\text{AUD}}_{i+\frac{1}{2}+} + h_{i+1}}{2} \tag{3.17}$$

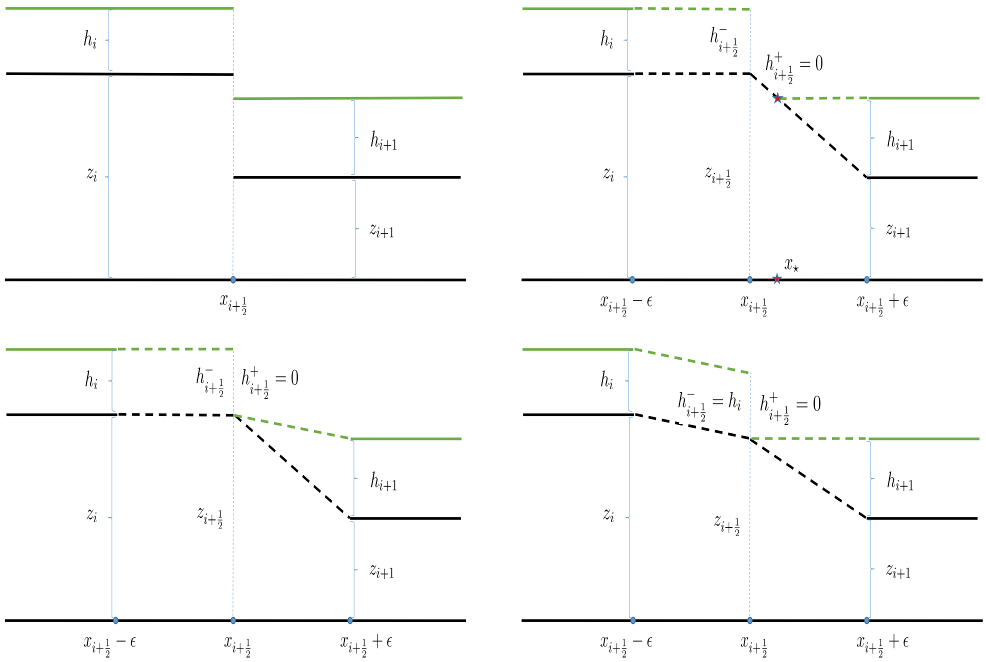

Figure 3: Subcell reconstruction of the water level in the partially dry case. top-left: Jump data; top-right: Audusse, or Morales for slow uphill flow; bottom-left: Morales for fast uphill flow; bottom-right: CN.

(ii) In the partially wet case, $h^{\mathrm{AUD}}_{i+\frac{1}{2}+}=0$ (see top-right of Figure 3). Assume that the wet-front is located at $x_\star \in \widehat{C}^{\varepsilon}_{i+\frac{1}{2}+}$. Then the average water height is

$$\overline{h}^{\mathrm{AUD}}_{i+\frac{1}{2}+} := \frac{1}{\varepsilon}\int_{\widehat{C}^{\varepsilon}_{i+\frac{1}{2}+}} h^{\mathrm{AUD}}_{\varepsilon}(x)\,dx \tag{3.18}$$

$$= \frac{x_{i+\frac{1}{2}}+\varepsilon-x_\star}{\varepsilon}\,\frac{h(x_\star)+h_{i+1}}{2} \tag{3.19}$$

$$= \frac{h_{i+1}}{z_{i+\frac{1}{2}}-z_{i+1}}\,\frac{h_{i+1}}{2} \tag{3.20}$$

where we have used the intercept theorem in the last equality. Summarizing (3.17) and (3.20), we obtain

$$\overline{h}^{\mathrm{AUD}}_{i+\frac{1}{2}+} = \begin{cases} \dfrac{h_{i+1}+h^{\mathrm{AUD}}_{i+\frac{1}{2}+}}{2}, & h^{\mathrm{AUD}}_{i+\frac{1}{2}+}>0, \\ \dfrac{h_{i+1}}{2}\,\dfrac{h_{i+1}}{z^{\mathrm{AUD}}_{i+\frac{1}{2}}-z_{i+1}}, & h^{\mathrm{AUD}}_{i+\frac{1}{2}+}=0. \end{cases} \tag{3.21}$$

Similarly,

$$\overline{h}^{\mathrm{AUD}}_{i+\frac{1}{2}-} = \begin{cases} \dfrac{h_{i}+h^{\mathrm{AUD}}_{i+\frac{1}{2}-}}{2}, & h^{\mathrm{AUD}}_{i+\frac{1}{2}-}>0, \\ \dfrac{h_{i}}{2}\,\dfrac{h_{i}}{z^{\mathrm{AUD}}_{i+\frac{1}{2}}-z_{i}}, & h^{\mathrm{AUD}}_{i+\frac{1}{2}-}=0. \end{cases} \tag{3.22}$$

3.3.2 The HR scheme of Morales et. al.

The continuous bottom of Morales' scheme coincides with that of the original HR scheme,

$$z_\varepsilon^{\mathrm{MOR}}(x) \equiv z_\varepsilon^{\mathrm{AUD}}(x). \tag{3.23}$$

The water level coincides with that of the original scheme, except for the partially wet interfaces (2.3): If the water flows downhill, or uphill with enough kinetic energy to climb the discrete jump of the bottom, i.e. (2.11) (respectively (2.13)) holds, then over $\hat{C}_{i+\frac{1}{2}-}$ (or $\hat{C}_{i+\frac{1}{2}+}$) the reconstructed water level $w_\varepsilon^{\mathrm{MOR}}(x)$ is given by the standard subcell reconstruction (see Definition 3.2) instead of Audusse' piecewise linear reconstruction (3.12) (see Figure 3). Then the local averages of $h_\varepsilon^{\mathrm{MOR}}(x)$ over subcells $\widehat{C}^\varepsilon_{i+\frac{1}{2}-}$ respectively $\hat{C}^\varepsilon_{i+\frac{1}{2}+}$ are simply

$$\overline{h}^{\mathrm{MOR}}_{i+\frac{1}{2}-} = \frac{h_i + h^{\mathrm{MOR}}_{i+\frac{1}{2}-}}{2} = \frac{h_i}{2} \quad \text{respectively} \quad \overline{h}^{\mathrm{MOR}}_{i+\frac{1}{2}+} = \frac{h_{i+1} + h^{\mathrm{MOR}}_{i+\frac{1}{2}+}}{2} = \frac{h_{i+1}}{2}, \tag{3.24}$$

since $h^{\mathrm{MOR}}_{i+\frac{1}{2}-} = 0$ $\big($respectively $h^{\mathrm{MOR}}_{i+\frac{1}{2}+} = 0\big)$.

3.3.3 The present HR scheme

The continuous bottom of our new scheme, $z_\varepsilon^{\mathrm{CN}}$, is defined by the standard subcell reconstruction with

$$z^{\mathrm{CN}}_{i-\frac{1}{2}+} := z^{\mathrm{CN}}_{i-\frac{1}{2}}, \quad z^{\mathrm{CN}}_{i+\frac{1}{2}-} := z^{\mathrm{CN}}_{i+\frac{1}{2}} \tag{3.25}$$

(see (2.15) for the pointvalues $z^{\mathrm{CN}}_{i+\frac{1}{2}}$). The reference values for the water surface are given by

$$w^{\mathrm{CN}}_{i-\frac{1}{2}+} := \min(w_i, z^{\mathrm{CN}}_{i-\frac{1}{2}} + h_i), \quad w^{\mathrm{CN}}_{i+\frac{1}{2}-} := \min(w_i, z^{\mathrm{CN}}_{i+\frac{1}{2}} + h_i), \tag{3.26}$$

and the reference values for the water depth are given by (2.16). Due to the linearity of $\widehat{h}_{i+\frac{1}{2}-}$ respectively $\widehat{h}_{i+\frac{1}{2}+}$, the average values of h_ε over the singular subcells $\widehat{C}^\varepsilon_{i-\frac{1}{2}+}$ respectively $\widehat{C}^\varepsilon_{i+\frac{1}{2}-}$ are

$$\overline{h}^{\mathrm{CN}}_{i-\frac{1}{2}+} = \frac{h_i + h^{\mathrm{CN}}_{i-\frac{1}{2}+}}{2} \quad \text{resp.} \quad \overline{h}^{\mathrm{CN}}_{i+\frac{1}{2}-} = \frac{h_i + h^{\mathrm{CN}}_{i+\frac{1}{2}-}}{2} \tag{3.27}$$

Remark 3.4. *From (3.21), (3.22) ,(3.24) and (3.27), the average of $h_\varepsilon(x)$ over subcells $\widehat{C}^\varepsilon_{i-\frac{1}{2}+}$ and $\widehat{C}^\varepsilon_{i+\frac{1}{2}-}$ obtained by the three schemes, $\overline{h}_{i-\frac{1}{2}+}$ and $\overline{h}_{i+\frac{1}{2}-}$ are in fact independent of ε.*

3.4 Fluxes and source terms based on subcell reconstructions

For all three hydrostatic schemes the flux vector is reconstructed by the standard subcell reconstruction (see Definition 3.2), with reference values

$$F_i := F(U_i), \quad F_{i+\frac{1}{2}-} := F_{i+\frac{1}{2}+} := F_{i+\frac{1}{2}} \tag{3.28}$$

where

$$F_{i+\frac{1}{2}} := \mathcal{F}_{\text{RIEM}}\Big(U_{i+\frac{1}{2}-}, U_{i+\frac{1}{2}+}\Big) \tag{3.29}$$

is an approximate Riemann solver. Note that the reconstructed flux $F_\varepsilon(x)$ is globally continuous. The definition of the reconstructed source term $S_\varepsilon(x) := \big(0, s_\varepsilon(x)\big)^T$ takes the natural form

$$s_\varepsilon(x) := -g\, h_\varepsilon(x)\, \partial_x z_\varepsilon(x) \tag{3.30}$$

and hence corresponds directly to (1.5).

Given (3.28) – (3.30) we now introduce the reconstructed, cell averaged residuum by

$$R_i^\varepsilon := -\frac{1}{\Delta x}\big(F_\varepsilon(x_{i+\frac{1}{2}}) - F_\varepsilon(x_{i-\frac{1}{2}})\big) + \frac{1}{\Delta x}\int\limits_{C_i} S(U_\varepsilon(x), z_\varepsilon(x))dx. \tag{3.31}$$

Depending on the choice of hydrostatic scheme, we denote the residuums by $R_i^{\varepsilon,\text{AUD}}$, $R_i^{\varepsilon,\text{MOR}}$ and $R_i^{\varepsilon,\text{CN}}$.

The key result of this section is the following theorem:

Theorem 3.5. *For each of the three hydrostatic schemes, and for each cell C_i, the reconstructed residuums are independent of ε, $R_i^\varepsilon = \overline{R}_i$ for all $\varepsilon > 0$, and coincide with the original definitions given in Section 2:*

$$\overline{R}_i^{AUD} = R_i^{AUD}, \tag{3.32}$$

$$\overline{R}_i^{MOR} = R_i^{MOR}, \tag{3.33}$$

$$\overline{R}_i^{CN} = R_i^{CN}. \tag{3.34}$$

Proof. First that the flux differences in (1.4) and (3.3) coincides. Therefore

$$\lim_{\varepsilon\to 0} R_i^\varepsilon - R_i = \Big(\lim_{\varepsilon\to 0}\frac{1}{\Delta x}\int\limits_{C_i} S(U_\varepsilon(x), z_\varepsilon(x))dx\Big) - S_i \tag{3.35}$$

$$= \big(0, \lim_{\varepsilon\to 0} s_i^\varepsilon - s_i\big)^T. \tag{3.36}$$

where

$$s_i^\varepsilon := \frac{-g}{\Delta x}\int\limits_{C_i} h_\varepsilon(x)\partial_x z_\varepsilon(x)dx \tag{3.37}$$

By the linearity of $z_\varepsilon(x)$,

$$\begin{aligned} s_i^\varepsilon &= -\frac{g}{\Delta x}\int\limits_{\hat{C}^\varepsilon_{i-\frac{1}{2}+}} h_\varepsilon(x)\partial_x z_\varepsilon(x)dx - \frac{g}{\Delta x}\int\limits_{\hat{C}^\varepsilon_{i+\frac{1}{2}-}} h_\varepsilon(x)\partial_x z_\varepsilon(x)dx \\ &= -\frac{g}{\Delta x}\frac{z_i - z_{i-\frac{1}{2}}}{\varepsilon}\int\limits_{\hat{C}^\varepsilon_{i-\frac{1}{2}+}} h_\varepsilon(x)dx - \frac{g}{\Delta x}\frac{z_{i+\frac{1}{2}} - z_i}{\varepsilon}\int\limits_{\hat{C}^\varepsilon_{i+\frac{1}{2}-}} h_\varepsilon(x)dx \\ &= -\frac{g}{\Delta x}\bar{h}_{i-\frac{1}{2}+}(z_i - z_{i-\frac{1}{2}}) - \frac{g}{\Delta x}\bar{h}_{i+\frac{1}{2}-}(z_{i+\frac{1}{2}} - z_i), \end{aligned} \tag{3.38}$$

which is independent of ε from Remark 3.4, so s_i^ε exists limit. It remains to show that for all three HR schemes,

$$\lim_{\varepsilon\to 0} s_i^\varepsilon - s_i = 0. \tag{3.39}$$

(i) Audusse' scheme. First we show that the first term on the RHS of (3.38) equals the left source term in the original HR scheme, as defined in (2.7), i.e we prove that

$$-\frac{g}{\Delta x}\bar{h}^{\rm AUD}_{i-\frac{1}{2}+}(z_i - z^{\rm AUD}_{i-\frac{1}{2}}) = \frac{g}{2\Delta x}((h_i)^2 - (h^{\rm AUD}_{i-\frac{1}{2}+})^2) \tag{3.40}$$

First suppose that $z^{\rm AUD}_{i-\frac{1}{2}} = z_i$. From (2.6)

$$h^{\rm AUD}_{i-\frac{1}{2}+} = \max(w_i - z^{\rm AUD}_{i-\frac{1}{2}}, 0) = \max(z_i + h_i - z_i, 0) = h_i.$$

Therefore both sides of (3.40) vanish in this case. Next, suppose that $z^{\rm AUD}_{i-\frac{1}{2}} = z_{i-1}$. Again from (2.6)

$$h^{\rm AUD}_{i-\frac{1}{2}+} = \max(w_i - z^{\rm AUD}_{i-\frac{1}{2}}, 0) = \max(z_i + h_i - z_{i-1}, 0)$$

If $h^{\rm AUD}_{i-\frac{1}{2}+} > 0$, then

$$-\frac{g}{\Delta x}\bar{h}^{\rm AUD}_{i-\frac{1}{2}+}(z_i - z^{\rm AUD}_{i-\frac{1}{2}}) = -\frac{g}{2\Delta x}(h_i + h^{\rm AUD}_{i-\frac{1}{2}+})(z_i - z_{i-1}) \tag{3.41}$$

$$= -\frac{g}{2\Delta x}(h_i + h^{\rm AUD}_{i-\frac{1}{2}+})(h^{\rm AUD}_{i-\frac{1}{2}+} - h_i) \tag{3.42}$$

which is the RHS of (3.40). If $h^{\rm AUD}_{i-\frac{1}{2}+} = 0$, then by (3.22)

$$-\frac{g}{\Delta x}\bar{h}^{\rm AUD}_{i-\frac{1}{2}+}(z_i - z^{\rm AUD}_{i-\frac{1}{2}}) = -\frac{g}{\Delta x}\frac{h_i}{2}\frac{h_i}{z_{i-1} - z_i}(z_i - z_{i-1}) = \frac{g(h_i)^2}{2\Delta x}, \tag{3.43}$$

which again coincides with the RHS of (3.40). The second term on the RHS of (3.38) can be treated analogously. This proves the theorem for Audusse' scheme.

(ii) The HR scheme of Morales et. al. This scheme differs the original HR scheme only when the water flows up a partially wet bottom. From (3.24) and (2.12) one can see immediately that

$$-\frac{g}{\Delta x}\bar{h}^{\rm MOR}_{i-\frac{1}{2}+}(z_i - z^{\rm MOR}_{i-\frac{1}{2}}) = -\frac{g}{\Delta x}\frac{h_i}{2}(z_i - z^{\rm MOR}_{i-\frac{1}{2}}) = s^{\rm MOR}_{i+\frac{1}{2}-}. \tag{3.44}$$

Similarly, one can see from (3.24) and (2.14) that

$$-\frac{g}{\Delta x}\bar{h}^{\rm MOR}_{i+\frac{1}{2}-}(z^{\rm MOR}_{i+\frac{1}{2}} - z_i) = -\frac{g}{\Delta x}\frac{h_i}{2}(z_i - z^{\rm MOR}_{i-\frac{1}{2}}) = s^{\rm MOR}_{i-\frac{1}{2}+}. \tag{3.45}$$

This finishes the proof of the theorem for Morales' scheme.

(iii) The present HR scheme. Using (3.27), we have

$$-\frac{g}{\Delta x}\bar{h}^{\rm CN}_{i-\frac{1}{2}+}(z_i - z^{\rm CN}_{i-\frac{1}{2}}) = -\frac{g}{\Delta x}\frac{h_i + h^{\rm CN}_{i-\frac{1}{2}+}}{2}(z_i - z^{\rm CN}_{i-\frac{1}{2}}) = s^{\rm CN}_{i-\frac{1}{2}+}$$

$$-\frac{g}{\Delta x}\bar{h}^{\rm CN}_{i+\frac{1}{2}-}(z^{\rm CN}_{i+\frac{1}{2}} - z_i) = -\frac{g}{\Delta x}\frac{h_i + h^{\rm CN}_{i+\frac{1}{2}-}}{2}(z^{\rm CN}_{i+\frac{1}{2}} - z_i) = s^{\rm CN}_{i-\frac{1}{2}+}.$$

This concludes the proof for the present scheme, and hence of Theorem 3.5. ∎

Remark 3.6. *(i) The subcell reconstructions offer a systematic approach to construct both known and also new HR schemes.*

(ii) The main advantage of the present scheme is its accuracy for shallow downhill flows. This can already be predicted from Figure 3: consider the bottom slope from z_i on the left to the water level w_{i+1} on the right. Does it contribute to an acceleration of the flow to the right? For Audusse' scheme it does not, since the water height $h_\varepsilon(x)$ in the subcell reconstruction is zero. For the present scheme however, the water height over this piece of downhill slope is $h_\varepsilon(x) \equiv h_i$, so

$$s^{CN}_{i+\frac{1}{2}-} = -\frac{g}{\Delta x} h_i (w_i - z_i).$$

This will be highlighted in the numerical experiments in Section 5.

4 Stability analysis

The present section establishes the stability of the new HR scheme: in Theorem 4.2, we prove positivity of the water height. In Theorem 4.5, we show that the scheme is well-balanced for the lake at rest. In Theorem 4.8, we establish a semi-discrete entropy inequality. The proofs are closely related to those in [Audusse et al., 2004]. Therefore, we begin our derivation with a detailed comparison of the three HR schemes.

Proposition 4.1 shows that the current HR scheme only differs from the previous methods in the partially wet case (2.3). Moreover, it differs only in $\overline{h}_{i+\frac{1}{2}\pm}$ and $z_{i+\frac{1}{2}}$.

Proposition 4.1. *For the above three HR schemes, we have that*

(i) *For all interfaces $x_{i+\frac{1}{2}}$,*

$$h^{AUD}_{i+\frac{1}{2}\pm} = h^{MOR}_{i+\frac{1}{2}\pm} = h^{CN}_{i+\frac{1}{2}\pm} \tag{4.1}$$

and

$$0 \le h_{i+\frac{1}{2}-} \le h_i, \qquad 0 \le h_{i+\frac{1}{2}+} \le h_{i+1} \tag{4.2}$$

(ii) *For fully wet interfaces $x_{i+\frac{1}{2}}$ (see (2.2)),*

$$z^{AUD}_{i+\frac{1}{2}} = z^{MOR}_{i+\frac{1}{2}} = z^{CN}_{i+\frac{1}{2}} \quad \text{and} \quad \overline{h}^{AUD}_{i+\frac{1}{2}\pm} = \overline{h}^{MOR}_{i+\frac{1}{2}\pm} = \overline{h}^{CN}_{i+\frac{1}{2}\pm} \tag{4.3}$$

(iii) *For partially wet interfaces $x_{i+\frac{1}{2}}$ (see (2.3)), and if water flows downhill, or it flows uphill with sufficient kinetic energy to climb the discrete jump of the bottom (i.e. neither (2.11) nor (2.13) holds), then*

$$z^{AUD}_{i+\frac{1}{2}} = z^{MOR}_{i+\frac{1}{2}} \quad \text{and} \quad \overline{h}^{AUD}_{i+\frac{1}{2}\pm} = \overline{h}^{MOR}_{i+\frac{1}{2}\pm}. \tag{4.4}$$

Proof. Morales' et al. [Morales de Luna et al., 2013] only modify the original HR scheme for downhill flows, or fast uphill flow according to either (2.11) or (2.13). So (iii) is proved and the relations between the original HR scheme and Morales' HR scheme in (i) and (ii) hold. Thus we only need to compare the original HR and the present HR schemes in (i) and (ii). There are two cases to be discussed:

(a) In the fully wet case (2.2),

$$\max(z_i, z_{i+1}) < \min(w_i, w_{i+1}), \tag{4.5}$$

so we have from (2.5) and (2.15),

$$z^{\mathrm{CN}}_{i+\frac{1}{2}} = z^{\mathrm{AUD}}_{i+\frac{1}{2}}. \tag{4.6}$$

Using (2.16) and (2.6),

$$h^{\mathrm{CN}}_{i+\frac{1}{2}-} = w_i - z_{i+\frac{1}{2}} = h^{\mathrm{AUD}}_{i+\frac{1}{2}-} \geq 0 \quad \text{and} \quad h^{\mathrm{CN}}_{i+\frac{1}{2}+} = w_{i+1} - z_{i+\frac{1}{2}} = h^{\mathrm{AUD}}_{i+\frac{1}{2}+} \geq 0. \tag{4.7}$$

Inserting this into (3.17) and (3.27), we obtain

$$\overline{h}^{\mathrm{CN}}_{i+\frac{1}{2}-} = \frac{h_i + h_{i+\frac{1}{2}-}}{2} = \overline{h}^{\mathrm{AUD}}_{i+\frac{1}{2}-} \quad \text{and} \quad \overline{h}^{\mathrm{CN}}_{i+\frac{1}{2}+} = \frac{h_i + h_{i+\frac{1}{2}+}}{2} = \overline{h}^{\mathrm{AUD}}_{i+\frac{1}{2}+}, \tag{4.8}$$

which proves (ii). And (i) holds for this case.

(b) It remains to prove (i) for the partially wet case (2.3). Without loss of generality suppose that

$$z_i \geq w_{i+1} \geq z_{i+1}. \tag{4.9}$$

For the original HR method,

$$z^{\mathrm{AUD}}_{i+\frac{1}{2}} = \max(z_i, z_{i+1}) = z_i. \tag{4.10}$$

Therefore,

$$h^{\mathrm{AUD}}_{i+\frac{1}{2}-} = \max(w_i - z^{\mathrm{AUD}}_{i+\frac{1}{2}}, 0) = h_i, \quad h^{\mathrm{AUD}}_{i+\frac{1}{2}+} = \max(w_{i+1} - z^{\mathrm{AUD}}_{i+\frac{1}{2}}, 0) = 0, \tag{4.11}$$

On the other hand, for the present HR method,

$$z^{\mathrm{CN}}_{i+\frac{1}{2}} = \min(\min(w_i, w_{i+1}), \max(z_i, z_{i+1})) = \min(w_{i+1}, z_i) = w_{i+1}, \tag{4.12}$$

so from (2.16)

$$h^{\mathrm{CN}}_{i+\frac{1}{2}-} = \min(w_i - z^{\mathrm{CN}}_{i+\frac{1}{2}}, h_i) = h_i, \quad h^{\mathrm{CN}}_{i+\frac{1}{2}+} = \min(w_{i+1} - z^{\mathrm{AUD}}_{i+\frac{1}{2}}, h_{i+1}) = 0. \tag{4.13}$$

Thus (i) is proved, and therefore the proposition. ■

In the following, we focus on the present HR scheme, and omit the superscript CN when there is no confusion. To simplify the proof, we use the well-known convex decomposition of the semi-discrete finite volume scheme (3.1),

$$\begin{aligned} \frac{d}{dt} U_i(t) = & R_{i-\frac{1}{2}+} + R_{i+\frac{1}{2}-} \\ := & -\frac{1}{\Delta x}\big(F_{i+\frac{1}{2}} - F(U_i)\big) + S_{i+\frac{1}{2}-} \\ & -\frac{1}{\Delta x}\big(F(U_i) - F_{i-\frac{1}{2}}\big) + S_{i-\frac{1}{2}+}. \end{aligned} \tag{4.14}$$

The next theorem states that our scheme preserves the positivity of the water height under the same condition as Audusse' scheme:

Theorem 4.2. *(Positivity) If the new semi-discrete HR scheme guarantees non-negative water height for the homogeneous shallow water equations, then it also yields non-negative water height for the shallow water equations with topography.*

Proof. As in [Audusse et al., 2004], we need to prove that if $h_i = 0$, then $R_{i-\frac{1}{2}+} \geq 0$ and $R_{i+\frac{1}{2}-} \geq 0$. Note that

$$U_{i-\frac{1}{2}+} = \begin{pmatrix} h_{i-\frac{1}{2}+} \\ h_{i-\frac{1}{2}+} u_{i-\frac{1}{2}+} \end{pmatrix} = \mathbf{0} \tag{4.15}$$

since $h_{i-\frac{1}{2}+} = 0$ due to (4.2). Let $U^{(1)}, F^{(1)}$ etc. be the first component of the vectors U, F etc.. Then

$$\begin{aligned} R^{(1)}_{i-\frac{1}{2}+} &= -\frac{1}{\Delta x}\left(F(U_i)^{(1)} - F^{(1)}_{i-\frac{1}{2}}\right) \\ &= -\frac{1}{\Delta x}\left(h_i u_i - \mathcal{F}_{\text{RIEM}}(U_{i-\frac{1}{2}-}, U_{i-\frac{1}{2}+})^{(1)}\right) \\ &= \frac{1}{\Delta x}\mathcal{F}_{\text{RIEM}}(U_{i-\frac{1}{2}-}, \mathbf{0})^{(1)} \end{aligned} \tag{4.16}$$

This expression is non-negative since the homogeneous finite volume scheme preserves non-negative water height. The same argument shows that $R_{i+\frac{1}{2}-} \geq 0$. This concludes the proof. ∎

Example 4.3. *To illustrate the last step in the proof of positivity, let us consider a Rusanov type flux [Rusanov, 1961] with maximal numerical wave speed $a_{i-\frac{1}{2}}$. Then*

$$\mathcal{F}_{RIEM}(U_{i-\frac{1}{2}-}, \mathbf{0}) = \frac{1}{2}\left(h_{i-\frac{1}{2}-}u_{i-\frac{1}{2}-} + h_{i-\frac{1}{2}+}u_{i-\frac{1}{2}+}\right) - \frac{a_{i-\frac{1}{2}}}{2}\left(h_{i-\frac{1}{2}+} - h_{i-\frac{1}{2}-}\right) \tag{4.17}$$

$$= \frac{1}{2}\left(h_{i-\frac{1}{2}-}u_{i-1}\right) + \frac{a_{i-\frac{1}{2}}}{2}h_{i-\frac{1}{2}-} \tag{4.18}$$

$$= \frac{1}{2}h_{i-\frac{1}{2}-}\left(u_{i-1} + a_{i-\frac{1}{2}}\right) \tag{4.19}$$

is non-negative under the CFL condition $a_{i-\frac{1}{2}} \geq \max(|u_{i-1}|, |u_i|)$.

Before we establish that our scheme is well-balanced, we would like to distinguish the following two classes of equilibria:

Definition 4.4. *(i) Given a constant water level w_{eq}, the* still water equilibrium *is given by $u(x) \equiv 0$ and*

$$h(x) + z(x) \equiv w_{eq} \tag{4.20}$$

The cell averages are consistent with the still water equilibrium, if for all i, $u_i = 0$ and

$$h_i + z_i = w_{eq}. \tag{4.21}$$

(ii) The lake-at-rest equilibrium *is given by $u(x) \equiv 0$ and*

$$h(x)\,\partial_x(h(x) + z(x)) \equiv 0. \tag{4.22}$$

for some constant $w_{eq} \geq \max_{x\in\mathbf{R}} z(x)$. Moreover, near a wet-dry interface, the dry part of z should not be lower than the adjecent water level.

The cell averages are locally *(at interface $x_{i+\frac{1}{2}}$)* consistent with the lake-at-rest*, if $u_i = u_{i+1} = 0$ and either $x_{i+\frac{1}{2}}$ is an interior interface (the still water case)*

$$h_i > 0,\ h_{i+1} > 0, \quad \textit{and} \quad h_i + z_i = h_{i+1} + z_{i+1} \tag{4.23}$$

or a dry-wet front

$$h_i = 0,\ h_{i+1} > 0 \quad \textit{and} \quad z_i \geq h_{i+1} + z_{i+1}, \tag{4.24}$$

or a wet-dry front

$$h_i > 0, h_{i+1} = 0, \quad \textit{and} \quad z_{i+1} \geq h_i + z_i, \tag{4.25}$$

or dry

$$h_i = h_{i+1} = 0. \tag{4.26}$$

The cell averages are globally consistent with the lake-at-rest*, if they are locally consistent with the lake-at-rest for all interfaces $x_{i+\frac{1}{2}}$.*

(iii) Suppose that the cell averages of the semi-discrete finite volume scheme (3.1) *are consistent with a given equilibrium state. Then we call the scheme* well-balanced *for this equilibrium state if $R_i = 0$ for all i.*

Theorem 4.5. *(Well-balancing) The present HR scheme is well-balanced for the lake at rest.*

Proof. By inspection, $R^{(1)}_{i+\frac{1}{2}-} = R^{(1)}_{i-\frac{1}{2}+} = 0$ for all interfaces. It remains to show that $R^{(2)}_{i+\frac{1}{2}-} = R^{(2)}_{i-\frac{1}{2}+} = 0$, as well.

(i) We begin with the interior interface (4.23). Here the flow is locally in still water equilibrium, and the interface $x_{i+\frac{1}{2}}$ is fully wet in the sense of (2.2). Therefore, our new scheme coincides with that of Audusse' et al., and

$$R^{(2)}_{i+\frac{1}{2}-} = \left(R^{\mathrm{AUD}}_{i+\frac{1}{2}-}\right)^{(2)} = 0. \tag{4.27}$$

(ii) Next, let us consider a dry-wet front as in (4.24). By (4.2), $h_{i+\frac{1}{2}-} = 0$. Thus from (3.27), $\overline{h}_{i+\frac{1}{2}-} = 0$. From (2.16), $h_{i+\frac{1}{2}+} = 0$ as well. Therefore, $U_{i+\frac{1}{2}-} = U_{i+\frac{1}{2}+} = \mathbf{0}$, and by consistency of the approximate Riemann solver, $F_{i+\frac{1}{2}} = F(\mathbf{0}) = \mathbf{0}$. Therefore, $R^{(2)}_{i+\frac{1}{2}-} = 0$.

Now we show that $R^{(2)}_{i+\frac{1}{2}+} = 0$. Note that

$$F(U_{i+1})^{(2)} = \frac{g}{2} h_{i+1}^2$$

and

$$\overline{h}_{i+\frac{1}{2}+} = \frac{h_{i+\frac{1}{2}+} + h_{i+1}}{2} = \frac{h_{i+1}}{2},$$

so

$$
\begin{aligned}
s_{i+\frac{1}{2}+} &= -\frac{g}{\Delta x}\frac{h_{i+1}}{2}(z_{i+1}-z_{i+\frac{1}{2}}) \\
&= -\frac{g}{\Delta x}\frac{h_{i+1}}{2}(z_{i+1}-(z_{i+1}+h_{i+1})) \\
&= \frac{g}{\Delta x}\frac{h_{i+1}^2}{2}.
\end{aligned} \tag{4.28}
$$

Therefore

$$
R^{(2)}_{i+\frac{1}{2}+} = -\frac{1}{\Delta x}F(U_{i+1})^{(2)} + s_{i+\frac{1}{2}+} = 0. \tag{4.29}
$$

(iii) The wet-dry case (4.25) can be treated analogously, and the dry case follows by inspection. ■

The remainder of this section is devoted to proving a semi-discrete entropy inequality for the new HR scheme. It is well-known (see e.g. [Bouchut, 2004]) that the shallow water equations with bottom source term, (1.1), admit the following entropy inequality, related to the physical energy:

$$
\partial_t \tilde{\eta}(U,z) + \partial_x \tilde{G}(U,z) \le 0. \tag{4.30}
$$

Here

$$
\tilde{\eta}(U,z) := \eta(U,z) + ghz \quad \text{and} \quad \tilde{G}(U,z) := G(U,z) + ghuz \tag{4.31}
$$

are the entropy respectively entropy-flux, which in turn are based on the entropy and entropy-flux for the homogeneous shallow water equations,

$$
\eta(U) := \frac{1}{2}hu^2 + \frac{1}{2}gh^2 \quad \text{and} \quad G(U) := \Big(\frac{1}{2}hu^2 + gh^2\Big)u. \tag{4.32}
$$

It is useful to write down the Jacobian of $\eta(U)$ and $\tilde{\eta}(U,z)$ with respect to U,

$$
\eta'(U) = \begin{pmatrix} gh - \frac{u^2}{2} \\ u \end{pmatrix}, \quad \tilde{\eta}'(U,z) = \eta'(U) + \begin{pmatrix} gz \\ 0 \end{pmatrix} \tag{4.33}
$$

Let us recall the classical semi-discrete entropy inequality:

Definition 4.6. *A semi-discrete scheme for the homogeneous problem,*

$$
\Delta x_i \frac{dU_i(t)}{dt} + \mathcal{F}(U_i, U_{i+1}) - \mathcal{F}(U_{i-1}, U_i) = 0, \tag{4.34}
$$

with numerical flux $\mathcal{F}$ consistent with $F(U)$ satisfies the **in-cell entropy inequality***, if there exists a numerical entropy flux $\mathcal{G}$ consistent with $G(U)$, such that*

$$
\Delta x_i \frac{d\eta(U_i(t))}{dt} + G(U_i, U_{i+1}) - G(U_{i-1}, U_i) \le 0. \tag{4.35}
$$

Before we prove a semi-discrete entropy inequality for the new HR scheme, we summarize some important results from [Audusse et al., 2004, Bouchut, 2004]. One can refine (4.35) by dividing each cell into two subcells. In [Bouchut, 2004, Lemma XY] it is proved that

(4.35) holds if and only if a corresponding entropy inequality holds to the left and right of each interface,

$$G(U_i) + \eta'(U_i)(\mathcal{F}(U_i, U_{i+1}) - F(U_i)) \geq \mathcal{G}(U_i, U_{i+1}) \tag{4.36}$$

$$\geq G(U_{i+1}) + \eta'(U_{i+1})(\mathcal{F}(U_i, U_{i+1}) - F(U_{i+1})). \tag{4.37}$$

To treat their HR scheme for the shallow water equations with source term, we use the shortcuts

$$F_{i+\frac{1}{2}} := \mathcal{F}(U_{i+\frac{1}{2}-}, U_{i+\frac{1}{2}+}) \quad \text{and} \quad G_{i+\frac{1}{2}} := \mathcal{G}(U_i, U_{i+1}, z_i, z_{i+1}). \tag{4.38}$$

In [Audusse et al., 2004, Bouchut, 2004], a numerical entropy flux $\tilde{G}$ for the inhomogeneous shallow water equations is introduced via

$$\tilde{G}_{i+\frac{1}{2}} := G_{i+\frac{1}{2}} + gF^h_{i+\frac{1}{2}} z_{i+\frac{1}{2}}. \tag{4.39}$$

The following lemma is at the heart of the matter:

Lemma 4.7. *[Audusse et al., 2004, Bouchut, 2004] The semi-discrete finite volume scheme (3.1) satisfies the semi-discrete entropy inequality*

$$\Delta x_i \frac{d}{dt} \tilde{\eta}(U_i(t), z_i) + \tilde{G}_{i+\frac{1}{2}} - \tilde{G}_{i-\frac{1}{2}} \leq 0. \tag{4.40}$$

if and only if

$$\tilde{G}(U_i, z_i) + \tilde{\eta}'(U_i, z_i)(F_{i+\frac{1}{2}} - \Delta x S_{i+\frac{1}{2}-} - F(U_i)) \geq \tilde{G}_{i+\frac{1}{2}} \tag{4.41}$$

$$\geq \tilde{G}(U_{i+1}, z_{i+1}) + \tilde{\eta}'(U_{i+1}, z_{i+1})(F_{i+\frac{1}{2}} + \Delta x S_{i+\frac{1}{2}+} - F(U_{i+1})) \tag{4.42}$$

Using this lemma, we now prove a semi-discrete entropy inequality for our new HR scheme:

Theorem 4.8. *(Entropy condition) Assume that the semi-discrete finite-volume scheme (4.34) for the homogeneous shallow water equation satisfies the in-cell entropy inequality (4.35) and that the numerical mass flux at the wet-dry front satisies*

$$\mathcal{F}^h(h, hu, 0, 0) - hu \geq 0, \qquad hu - \mathcal{F}^h(0, 0, h, hu) \geq 0. \tag{4.43}$$

Then the semi-discrete HR scheme (3.1) satisfies the entropy inequality (4.40) for the inhomogeneous shallow water equation.

Proof: According to Lemma 4.7, we need to prove the two inequalities (4.41) - (4.42) for the new HR scheme. Due to symmetry, we focus on (4.41). Substracting the two sides, we introduce the entropy production term

$$\tilde{E}_{i+\frac{1}{2}-} := \tilde{\eta}'(U_i, z_i)(-F_{i+\frac{1}{2}} + F(U_i) + \Delta x S_{i+\frac{1}{2}-}) + \tilde{G}_{i+\frac{1}{2}} - \tilde{G}(U_i, z_i). \tag{4.44}$$

Our goal is to show that $\tilde{E}_{i+\frac{1}{2}-} \leq 0$. Using (4.33) and

$$\Delta x S_{i+\frac{1}{2}-} = \left(0, -g\bar{h}_{i+\frac{1}{2}-}(z_{i+\frac{1}{2}} - z_i)\right)^T \tag{4.45}$$

we compute

$$\begin{aligned}
\tilde{E}_{i+\frac{1}{2}-} &= \tilde{\eta}'(U_i,z_i)(-F_{i+\frac{1}{2}}+F(U_i)) - u_i g\bar{h}_{i+\frac{1}{2}-}(z_{i+\frac{1}{2}}-z_i)\\
&\quad + G_{i+\frac{1}{2}} + gF^h_{i+\frac{1}{2}-}z_{i+\frac{1}{2}} - G(U_i) - gh_iu_iz_i\\
&= \eta'(U_i)(-F_{i+\frac{1}{2}}+F(U_i)) + G_{i+\frac{1}{2}} - G(U_i)\\
&\quad + gz_i(-F^h_{i+\frac{1}{2}} + h_iu_i)\\
&\quad + g\big(F^h_{i+\frac{1}{2}-} - \bar{h}_{i+\frac{1}{2}-}u_i\big)z_{i+\frac{1}{2}} - g\big(h_iu_i - \bar{h}_{i+\frac{1}{2}-}u_i\big)z_i\\
&= \eta'(U_i)(-F_{i+\frac{1}{2}}+F(U_i)) + G_{i+\frac{1}{2}} - G(U_i)\\
&\quad + g\big(F^h_{i+\frac{1}{2}-} - \bar{h}_{i+\frac{1}{2}-}u_i\big)(z_{i+\frac{1}{2}}-z_i).
\end{aligned} \tag{4.46}$$

Now we evaluate (4.36) at $(U_{i+\frac{1}{2}-}, U_{i+\frac{1}{2}+})$ instead of (U_i, U_{i+1}),

$$G_{i+\frac{1}{2}} \le \eta'(U_{i+\frac{1}{2}-})\big(F_{i+\frac{1}{2}} - F(U_{i+\frac{1}{2}-})\big) + G(U_{i+\frac{1}{2}-}) \tag{4.47}$$

and insert this into (4.46) to obtain

$$\begin{aligned}
\tilde{E}_{i+\frac{1}{2}-} &\le \eta'(U_i)(-F_{i+\frac{1}{2}}+F(U_i)) - G(U_i)\\
&\quad + g\big(F^h_{i+\frac{1}{2}-} - \bar{h}_{i+\frac{1}{2}-}u_i\big)(z_{i+\frac{1}{2}}-z_i)\\
&\quad + \Big(\eta'(U_{i+\frac{1}{2}-})\big(F_{i+\frac{1}{2}} - F(U_{i+\frac{1}{2}-})\big) + G(U_{i+\frac{1}{2}-})\Big)\\
&=: \tilde{E}^A_{i+\frac{1}{2}-}.
\end{aligned} \tag{4.48}$$

Using the identities

$$G(U) - \eta'(U)F(U) = (\frac{1}{2}hu^2 + gh^2)u - \big((gh - \frac{u^2}{2})hu + u(hu^2 + \frac{1}{2}gh^2)\big) = -\frac{1}{2}gh^2u$$

and

$$\eta'(U_i) - \eta'(U_{i+\frac{1}{2}-}) = \begin{pmatrix} gh_i - \frac{(u_i)^2}{2} \\ u_i \end{pmatrix} - \begin{pmatrix} gh_{i+\frac{1}{2}-} - \frac{(u_i)^2}{2} \\ u_i \end{pmatrix} = \begin{pmatrix} g(h_i - h_{i+\frac{1}{2}-}) \\ 0 \end{pmatrix}$$

we calculate

$$\begin{aligned}
\tilde{E}^A_{i+\frac{1}{2}-} &= \frac{1}{2}g((h_i)^2 - (h_{i+\frac{1}{2}-})^2)u_i - g(h_i - h_{i+\frac{1}{2}-})F^h_{i+\frac{1}{2}} + g(F^h_{i+\frac{1}{2}} - u_i\bar{h}_{i+\frac{1}{2}-})(z_{i+\frac{1}{2}}-z_i)\\
&= g\Big(F^h_{i+\frac{1}{2}} - \frac{h_{i+\frac{1}{2}-}+h_i}{2}u_i\Big)(h_{i+\frac{1}{2}-} - h_i) + g(F^h_{i+\frac{1}{2}} - \bar{h}_{i+\frac{1}{2}-}u_i)(z_{i+\frac{1}{2}}-z_i)
\end{aligned} \tag{4.49}$$

For the present scheme, according to (3.17), (3.25) and (3.27), we have

$$\bar{h}_{i+\frac{1}{2}-} = \frac{h_i + h_{i+\frac{1}{2}-}}{2} \tag{4.50}$$

then $E^A_{i+\frac{1}{2}-}$ becomes

$$\tilde{E}^A_{i+\frac{1}{2}-} = g\big(F^h_{i+\frac{1}{2}} - \bar{h}_{i+\frac{1}{2}-}u_i\big)\big((h_{i+\frac{1}{2}-} + z_{i+\frac{1}{2}}) - (h_i + z_i)\big) \tag{4.51}$$

Our goal is to show that $\tilde{E}^A_{i+\frac{1}{2}-} \leq 0$. There are two cases to be discussed:

(i) In the fully wet case (see (2.2)), $\min(w_i, w_{i+1}) > \max(z_i, z_{i+1})$. According to (2.15) and (3.27), we have

$$z_{i+\frac{1}{2}} + h_{i+\frac{1}{2}-} = h_i + z_i \tag{4.52}$$

then

$$\tilde{E}^A_{i+\frac{1}{2}-} = 0. \tag{4.53}$$

(ii) In the partially wet case (see (2.3)), $\min(w_i, w_{i+1}) \leq \max(z_i, z_{i+1})$. There are two sub-cases depending on whether left bottom is higher than the right bottom. We first consider $z_i > z_{i+1}$. According to (3.9), (3.25), (3.26) and (3.27),

$$z_{i+\frac{1}{2}} = w_{i+1},\ h_{i+\frac{1}{2}-} = h_i,\ h_{i+\frac{1}{2}+} = 0 \text{ and } \overline{h}_{i+\frac{1}{2}-} = h_i. \tag{4.54}$$

Therefore,

$$\tilde{E}^A_{i+\frac{1}{2}-} = g(\mathcal{F}(h_i, h_i u_i, 0, 0) - h_i u_i)(w_{i+1} - z_i) \tag{4.55}$$

By (2.3), $w_{i+1} - z_i < 0$, and due to (4.43), $\mathcal{F}(h_i, h_i u_i, 0, 0) - h_i u_i) \geq 0$. This implies that $\tilde{E}_{i+\frac{1}{2}-} \leq 0$.

Next we consider the case $z_i < z_{i+1}$. Analogously to (4.54),

$$z_{i+\frac{1}{2}} = w_i,\ h_{i+\frac{1}{2}-} = 0,\ h_{i+\frac{1}{2}+} = h_{i+1}, \text{ and } \overline{h}_{i+\frac{1}{2}-} = \frac{1}{2} h_i. \tag{4.56}$$

Therefore,

$$z_{i+\frac{1}{2}} + h_{i+\frac{1}{2}-} = h_i + z_i \tag{4.57}$$

then

$$\tilde{E}^A_{i+\frac{1}{2}-} = 0. \tag{4.58}$$

∎

Let us discuss condition (4.43)

Remark 4.9. *For a finite volume, some diffusion terms are always added to the numerical flux. To preserve the positivity, The diffusion must be large enough such that*

$$\mathcal{F}^h(0, 0, h, hu)) \leq 0, \qquad \mathcal{F}^h(h, hu, 0, 0)) \geq 0 \tag{4.59}$$

and always (but not necessary) (4.43) holds, which will be proved for Harten van-Leer Lax (HLL) flux,

$$\begin{aligned}\mathcal{F}(U_-, U_+) &= \frac{s^+ F(U_-) - s^- F(U_+) + s^+ s^- (U_+ - U_-)}{s^+ - s^-} \\ &= \frac{-s^- F(U_+) + s^- s^+ U_+}{s^+ - s^-} + \frac{s^+ F(U_-) - s^+ s^- U_-}{s^+ - s^-}\end{aligned} \tag{4.60}$$

where the smallest and largest wave speeds s^- and s^+ are chosen as

$$s^- = \min(u_- - a_-, u_+ - a_-, 0), \quad s^+ = \max(u_- + a_-, u_+ + a_+, 0). \tag{4.61}$$

with the sound speed $a = \sqrt{gh}$. Then we have

$$\begin{aligned} \mathcal{F}^h(h, hu, 0, 0) - hu &= \frac{s^+ hu - s^+ s^- h}{s^+ - s^-} - hu = \frac{-s^- h(s^+ - u)}{s^+ - s^-} \geq 0, \\ hu - \mathcal{F}^h(0, 0, h, hu) &= hu - \frac{-s^- hu + s^+ s^- h}{s^+ - s^-} = \frac{s^+ h(u - s^-)}{s^+ - s^-} \geq 0. \end{aligned}$$

Then (4.43) holds, so the entropy theorem 4.8 holds.

5 Numerical experiments

In this section, we present several numerical experiments to test the new HR scheme. After verifying that all three schemes preserve the lake-at-rest (Section 5.1), we study three cases of downhill flow which clearly show the advantages of the new HR scheme. The first case (Section 5.2) is a thin layer of water running down a linear slope. We give an analysis of a prototype situation which clearly explains the differences of the three schemes. The second case (Section 5.3) is flow over a step. The third case is a vacuum Riemann problem over constant bottom, followed by a downward step (Section 5.4).

The next group of tests shows upward flow (Section 5.5) and twodimensional flow (Section 5.6). Here our scheme performs comparably to the other HR schemes.

We discretize the semi-discrete finite volume scheme (1.3) in time using the forward Euler method. This yields

$$U_i^{n+1} = U_i^n + \Delta t R_i^n. \tag{5.1}$$

The time step is restricted by the CFL condition

$$\frac{\Delta t}{\Delta x} \max_i (|u_i| + a_i) < \frac{1}{2}. \tag{5.2}$$

5.1 Still water flow over a complex bottom

First we validate numerically that the new scheme preserves the lake at rest (including dry areas according to Definition 4.4). The bottom topography is given by

$$z(x) = \begin{cases} \sin(4\pi x), & x \leq 0.5, \\ \sin(4\pi x) - 2.0, & x \geq 0.5. \end{cases}$$

and the initial data are

$$h(x, t=0) = \begin{cases} \max(0, -0.5 - z(x)), & x \leq 0.5 \\ \max(0, -1.5 - z(x)), & x \geq 0.5. \end{cases}, \quad u(x, t=0) = 0.$$

The numerical solutions computed by the three HR schemes with 50 cells and final time $t = 0.5$ are shown in Figure 4. All schemes are well-balanced up to machine accuracy.

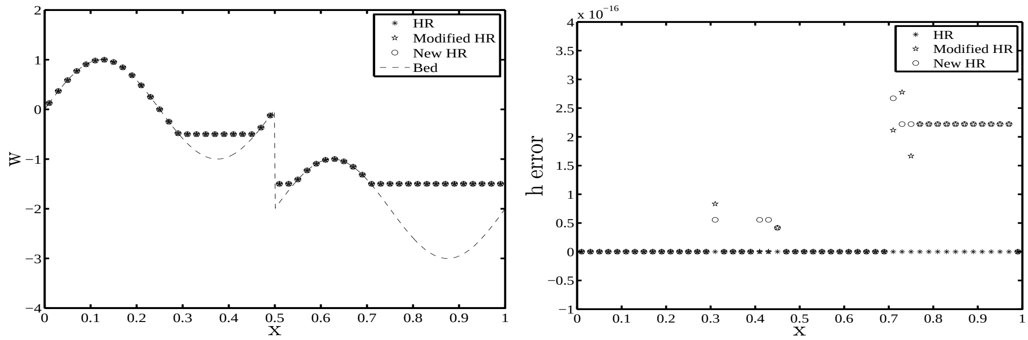

Figure 4: Still water flow over a complex bottom. Left: the surface w; Right: the error of the water hight h. The domain is divided into 50 uniform cells.

5.2 Downhill flow over a sloped bottom

This test problem was introduced by Delestre et al. [Delestre et al., 2012] to demonstrate a subtle difficulty of Audusse' original HR scheme. It was subsequently used by Morales et al. [Morales de Luna et al., 2013] to demonstrate the advantage of a modified HR scheme.

The bottom is defined by

$$z(x) = -\frac{\alpha}{100}x$$

in the interval $[0,3]$ for different values of slope α ranging from 16 to 21. The initial condition is

$$h(x,t=0) = 0.02, \quad u(x,t=0) = 0.5.$$

The left inflow boundary is given by setting $h(x=0,t)=0.02$ and $u(x=0,t)=0.5$, and an outflow flow boundary condition is imposed at the right boundary $x=3$. The simulations are performed until a steady state is reached at time $t=10$.

As observed in [Delestre et al., 2012], the water height of the HR scheme remains independent of the slope (see upper-left plot in Figure 5). This is contrary to the physical solution, for which the water level decreases with increasing downhill slope. The results for the modified HR scheme (upper-right plot) and the present scheme (lower left plot) depend on the slope, but in slightly different ways. In the lower-right plot, we compare the three schemes with a resolved reference solution for $\alpha=21$. The advantages of the modified and especially the new HR schemes are clearly visible.

The following argument, along the lines of Remark 3.6, illuminates the situation. Let

$$S_{i+\frac{1}{2}} := S_{i+\frac{1}{2}-} + S_{i+\frac{1}{2}+} \tag{5.3}$$

be the total source term at interface $x_{i+\frac{1}{2}}$. Suppose that the slope is downward, $z_x < 0$, and the water heigth h is constant. The exact source term is given by

$$S^{\text{ex}}_{i+\frac{1}{2}} = -\frac{g}{\Delta x}\int_{x_i}^{x_{i+1}} h z_x \, dx = -g h z_x. \tag{5.4}$$

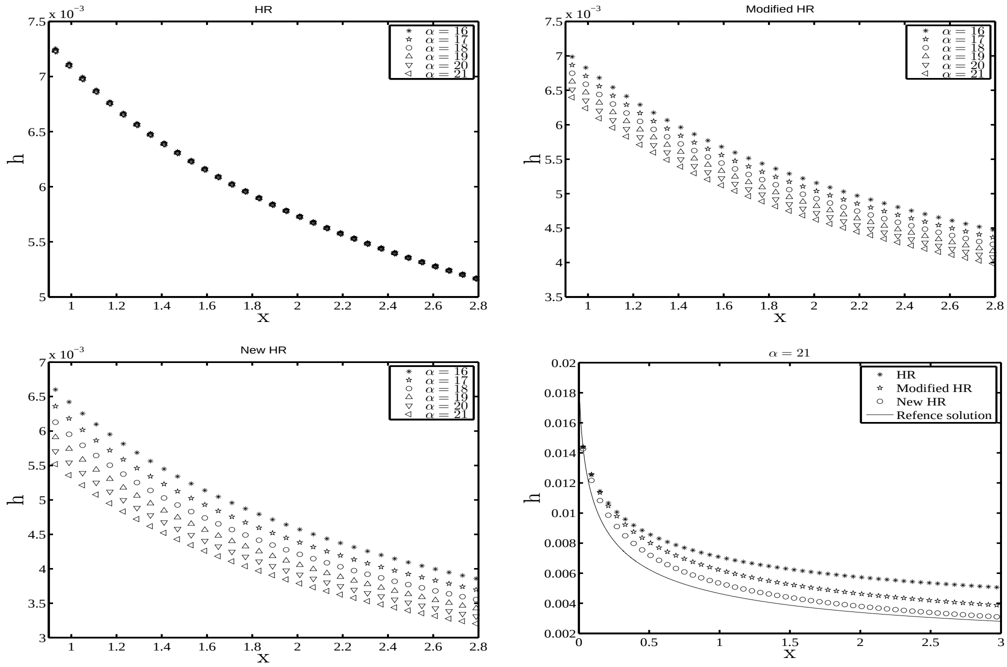

Figure 5: Water flow with $h_l = 0.02$ and $u_l = 0.5$ over sloped bottom. Top left: HR; top-right: modified HR; lower-left: new HR (all using 50 cells and $\alpha = 16 \ldots 21$). Lower-right: comparison with the reference solution for $\alpha = 21$.

In the fully wet case (labeled "fw" below), where all schemes coincide, (2.7) – (2.8) give

$$\begin{aligned} S^{\text{fw}}_{i+\frac{1}{2}} &= \frac{g}{2\Delta x}\big((h^{\text{AUD}}_{i+\frac{1}{2}-})^2 - (h_i)^2 + (h_{i+1})^2 - (h^{\text{AUD}}_{i+\frac{1}{2}+})^2\big) \\ &= -\frac{g}{\Delta x} h_{i+1}(z_{i+1} - z_i) - \frac{g}{2\Delta x}(z_{i+1} - z_i)^2 \\ &= S^{\text{ex}}_{i+\frac{1}{2}} - \frac{\Delta x\, g}{2} z_x^2 \end{aligned} \tag{5.5}$$

In the partially wet case ($h < \Delta x |z_x|$), using (2.7) – (2.8) for Audusse' scheme, (2.14) for Morales' modification, and (2.17) – (2.18) for the present scheme, we obtain

$$\begin{aligned} S^{\text{AUD}}_{i+\frac{1}{2}} &= \frac{g}{2\Delta x}(h_{i+1})^2 = \frac{g}{2\Delta x} h^2, \\ S^{\text{MOR}}_{i+\frac{1}{2}} &= -\frac{g}{2\Delta x} h_{i+1}\big(z_{i+1} - z^{\text{MOR}}_{i+\frac{1}{2}}\big) = -\frac{g}{2} h\, z_x, \\ S^{\text{CN}}_{i+\frac{1}{2}} &= -\frac{g}{2\Delta x}\Big((h_i + h^{\text{CN}}_{i+\frac{1}{2}-})\big(z^{\text{CN}}_{i+\frac{1}{2}} - z_i\big) + (h^{\text{CN}}_{i+\frac{1}{2}+} + h_{i+1})\big(z_{i+1} - z^{\text{CN}}_{i+\frac{1}{2}}\big)\Big) \\ &= -\frac{g}{2\Delta x}\Big(2h_i\big(z_{i+1} + h_{i+1} - z_i\big) + h_{i+1}\big(-h_{i+1}\big)\Big) \\ &= S^{\text{ex}}_{i+\frac{1}{2}} - \frac{g}{2\Delta x} h^2. \end{aligned} \tag{5.6}$$

It is instructive to introduce the ratio of the water height over the height increment,

$$\beta := h/(\Delta x |z_x|).$$

Then in the fully wet case,

$$S^{\text{fw}}_{i+\frac{1}{2}} / S^{\text{ex}}_{i+\frac{1}{2}} = 1 - \frac{1}{2\beta}, \tag{5.7}$$

which tends to the optimal value of unity for deep water, while in the partially wet cases,

$$
\begin{aligned}
S^{\mathrm{AUD}}_{i+\frac{1}{2}}/S^{\mathrm{ex}}_{i+\frac{1}{2}} &= \frac{\beta}{2},\\
S^{\mathrm{MOR}}_{i+\frac{1}{2}}/S^{\mathrm{ex}}_{i+\frac{1}{2}} &= \frac{1}{2},\\
S^{\mathrm{CN}}_{i+\frac{1}{2}}/S^{\mathrm{ex}}_{i+\frac{1}{2}} &= 1-\frac{\beta}{2}.
\end{aligned}
\tag{5.8}
$$

Only for the present HR scheme this fraction tends to the correct value of unity as the water height ends to zero. The values S/S^{ex} are displayed versus β in Figure 6.

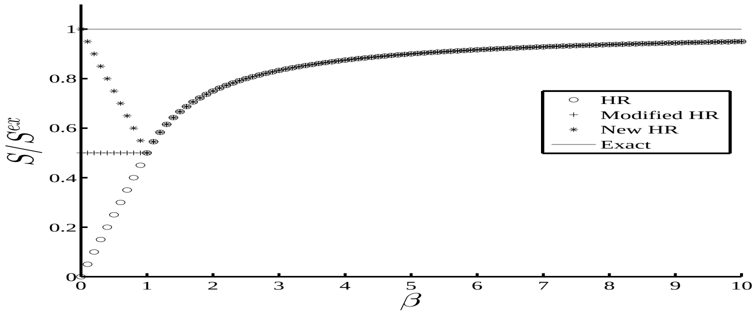

Figure 6: S/S^{ex} for the exact source term ('-'), the original HR ('o'), modified HR ('+'), and new HR ('*'). Only the latter is consistent as $\beta \to 0$.

In the present experiment, β is not constant, but its value is approximately

$$\beta \approx \frac{0.01}{\frac{3}{50}\frac{20}{100}} = \frac{5}{6}.$$

To highlight the difference of the three schemes even further, we repeat the experiment with a value $\beta \approx \frac{1}{6}$, by setting the initial water height to $h=0.004$. The results are displayed in Figure 7. As can be seen from the lower right part of the figure, the new HR scheme produces almost the exact solution on a grid of 50 cells, while the other two schemes do not.

5.3 Flow over a step

This test was introduced in [Castro et al., 2008, Morales de Luna et al., 2013]. In the previous example, the bottom was continuous, and the fault of the hydrostatic reconstruction scheme could be corrected by using a very fine mesh or higher order schemes.

In this example, we consider the domain $[0,1]$ with a discontinuous bottom given by

$$b(x) = \begin{cases} -0.1 & \text{for } x < 0.5 \\ b_r & \text{otherwise} \end{cases}.$$

The constant topography b_r to the right of the step takes decreasing values from -0.2 to -0.45, respectively. The initial data are set to

$$h(x,t=0) = 0.1, \quad u(x,t=0) = 1.5.$$

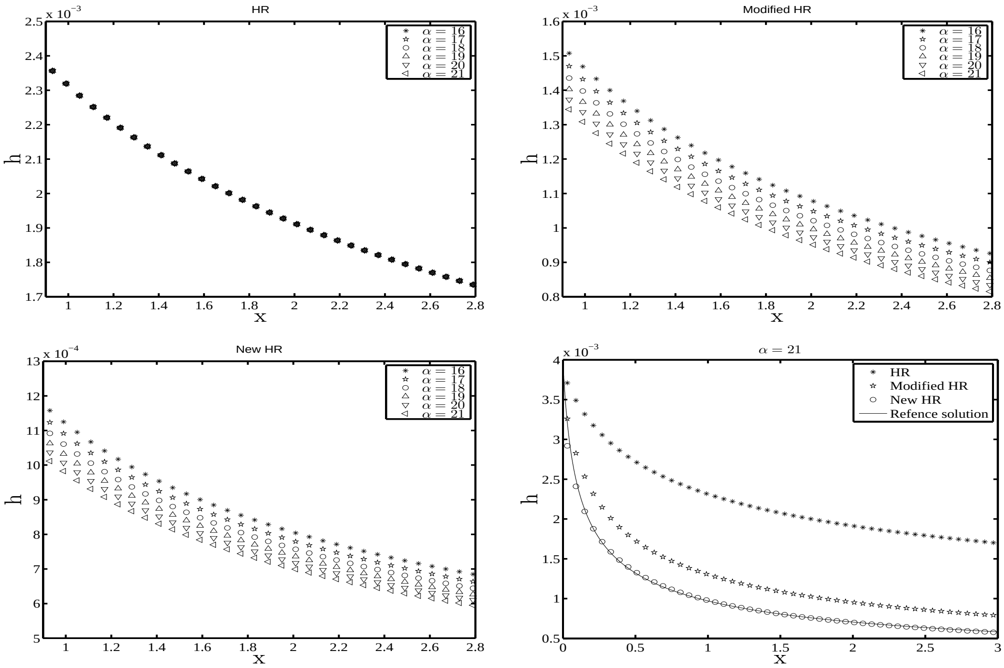

Figure 7: Water flow with $h_l = 0.004$ and $u_l = 0.5$ over sloped bottom. Top left: HR; top-right: modified HR; lower-left: new HR (all using 50 cells and $\alpha = 16 \ldots 21$). Lower-right: comparison with the reference solution for $\alpha = 21$.

uniformly over the whole domain. The final time is $t = 3.0$.

It is easy to check that the interface at the discontinuity is partially dry, so Audusse' source term depends only on the waterlevel to the right of the step, and not on the step size $b_r - b_l$. This is confirmed by the numerical results displayed in the top-left plot in Figure 8, which do not differ as the step size varies. Clearly, this does not reflect the increasing gravitational acceleration correctly.

The next two sub-figures show that the error produced by the original HR method is corrected by both the modified HR method and the new HR method. As shown in the two sub-figures, the lower the right bottom b_r is, the lower the water depth in the right region is. On the other hand, we can also see the these two sub figures, the numerical results done by the two schemes are different, it is clear the right water depth by the new HR method is lower than that done by modified HR method.

Remark 5.1. *To compare the two result, we need a reference solution. Ideally this reference solution should not be affected by the non-uniquness due to the non-conservative product (1.5). An important result in this direction is due to Audusse et al. [Audusse et al., 2004], who derive a semi-discrete entropy condition for the HR method if the bottom jump is of the order of the mesh size Δx. It is to be expected that this solution is unique. Motivated by this, we replace the jump by a continuous transition of width ε and then resolve the transition layer with a sufficiently fine grid (usually 100 cells). For the present flow over a step, we choose*

$$b_\varepsilon(x) = \begin{cases} -0.1 & \textit{for } x < 0.5, \\ -0.1 + \frac{x-0.5}{\varepsilon}(b_r + 0.1) & \textit{for } 0.5 \le x \le 0.5 + \varepsilon, \\ b_r & \textit{otherwise}, \end{cases}$$

with layer width $\varepsilon = 10^{-2}$ and 10^4 cells. Therefore, there are 100 cells in the layer.

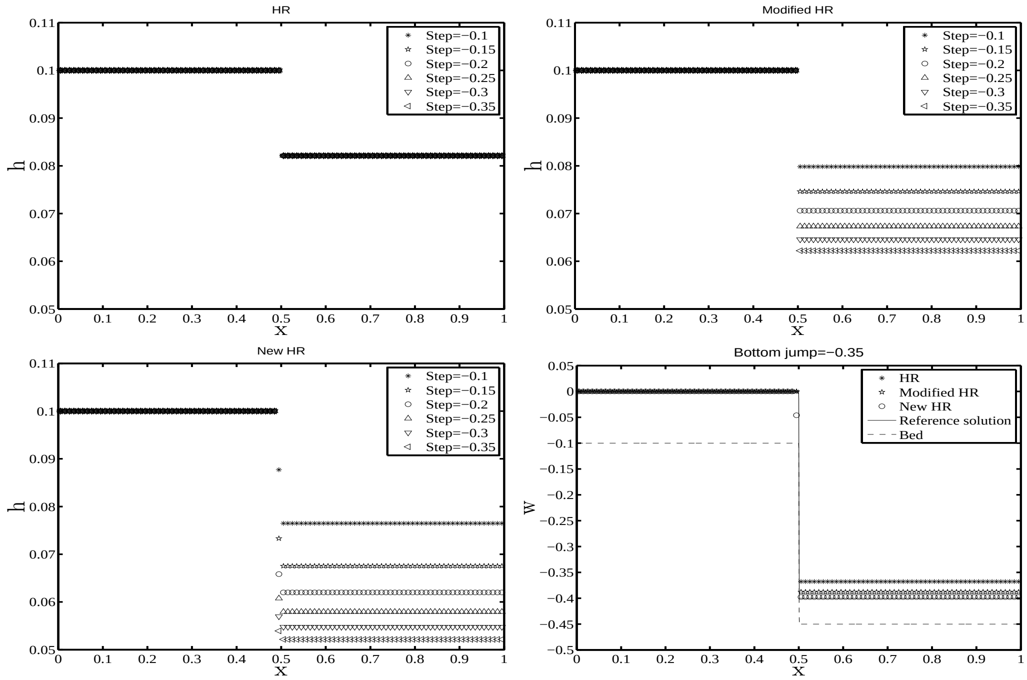

Figure 8: Downhill flow over a step. Water depths computed with HR (top-left), modified HR (top-right) and new HR (lower-left) schemes with several different bottom steps and 100 cells; bottom-right: water levels of the three schemes compared with the reference solution.

The results of the three schemes for right bottom $b_r = -0.45$ are shown in the lower-right sub-figure. We can see that all the three results are higher than the reference solution. Compared with the size of the jump, the error of the three HR schemes are 9.1%, 3.4% and 0.6%, respectively.

5.4 Dam break over a dry step

Here we consider a dam-break over a dry bottom, combined with a bottom step to the right of the dam break. Compared with the previous problem, the additional difficulty is the wet-dry front propagating to the right. This problem has been considered in [Castro et al., 2008, Bollermann et al., 2013]. The domain is [0,1], and the bottom is defined by

$$b(x) = \begin{cases} -0.1 & \text{for } x < 0.1 \\ -0.45 & \text{otherwise} \end{cases}$$

The initial data are

$$u(x) = 0, \quad h(x) = \begin{cases} 0.5 & \text{for } x < 0.05, \\ 0 & \text{otherwise.} \end{cases}$$

The final time is $t=0.18$. As motivated in Remark 5.1, the reference solution is computed over the steep continuous topography

$$b_\varepsilon(x) = \begin{cases} -0.1 & \text{for } x<0.1, \\ -0.1-0.35\,\frac{x-0.1}{\varepsilon} & \text{for } 0.1 \le x \le 0.1+\varepsilon, \\ -0.45 & \text{otherwise} \end{cases}$$

with $\varepsilon = 10^{-3}$ and 10^5 cells.

In Figure 9, we display the front position, velocity history as well as the solutions at the final time using 400 cells. While the fronts computed by all three schemes lag behind the reference solution, the new HR scheme clearly is superior to the previous ones at and away from the front.

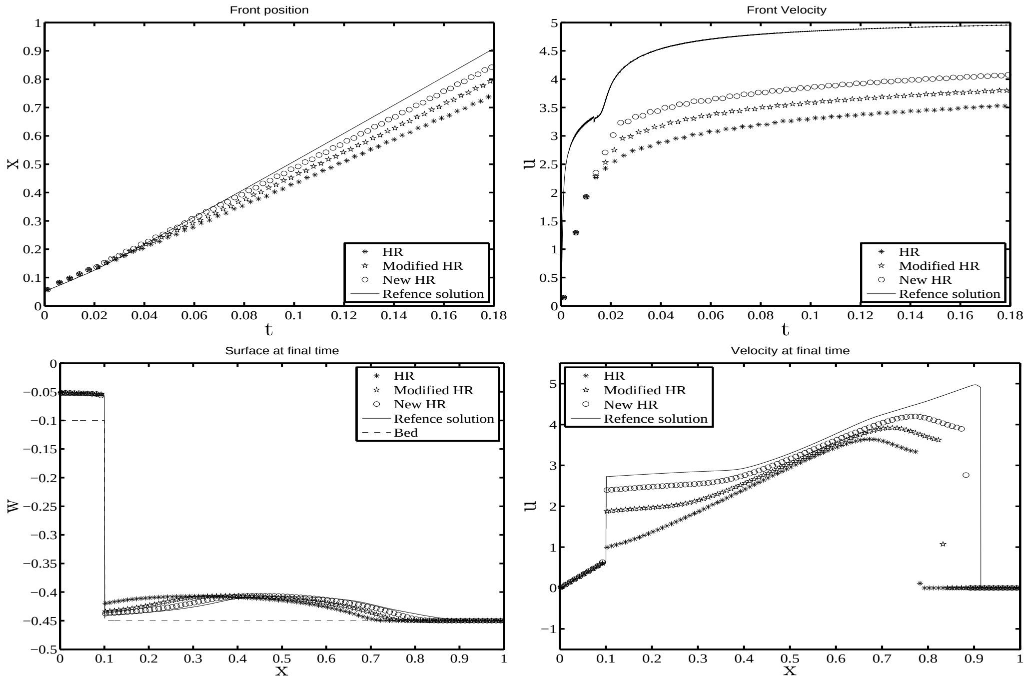

Figure 9: Dam-break problem over dry bottom with an abrupt valley. The front position and velocity histories; The water height h and velocity u.

5.5 Flow against a step

Here we consider flow towards, and sometimes over, a rising step [Morales de Luna et al., 2013]. From our derivation, there is no particular reason that the new HR scheme should be superior to the previous ones, and indeed our experiments only confirm that the performance is comparable.

We consider the domain $[-5,5]$ and a series of test cases with steps of various decreasing heights,

$$b(x) = \begin{cases} -0.8 & \text{for } x<0.5 \\ b_r & \text{otherwise} \end{cases},$$

where $b_r = -0.4, -0.5, -0.65, -0.75$ respectively. The initial height and velocity are constant

$$h(x,t=0)=0.1, \quad u(x,t=0)=1.5 \quad \text{for all } x\in[-5,5].$$

The final time is $t=4.5, 3.5, 2.0, 5.0$ respectively. As discussed in Remark 5.1, the reference solution is computed over the steep continuous topography

$$b_\varepsilon(x)=\begin{cases} -0.8 & \text{for } x<0.5,\\ -0.8+\frac{x-0.5}{\varepsilon}(b_r+0.8) & \text{for } 0.5\le x\le 0.5+\varepsilon,\\ b_r & \text{otherwise },\end{cases}$$

with 10^5 cells and $\varepsilon=10^{-2}$.

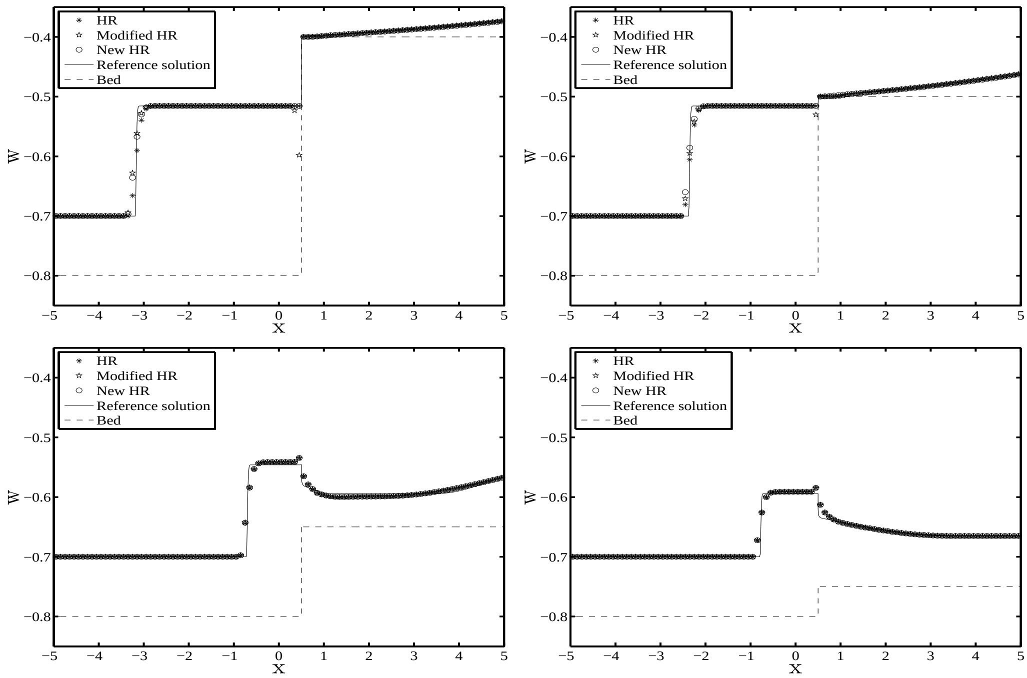

Figure 10: Flow against a step: Water levels corresponding to $b_r=-0.4$, -0.5, -0.65, and -0.75.

The numerical results for the three HR schemes with 100 cells are shown in Figure 10. The four sub-figures are corresponding to the four different bottoms. Indeed, from (2.11),

$$\frac{|u_i|^2}{2}+g(w_i-b_r^*)=\frac{3}{2}\sqrt{g(h_i|u_i|)^3}. \tag{5.9}$$

or

$$\frac{|u_i|^2}{2}+gw_i=\frac{3}{2}\sqrt{g(h_i|u_i|)^3}+gb_r^*. \tag{5.10}$$

or

$$gb_r^*=\frac{|u_i|^2}{2}+gw_i-\frac{3}{2}\sqrt{g(h_i|u_i|)^3} \tag{5.11}$$

$$=\frac{1.5^2}{2}+g(-0.8+0.1)-\frac{3}{2}\sqrt{g(0.1\cdot 1.5)^3} \tag{5.12}$$

For all cases, the HR method and new HR method give a similar results, which are very close to the reference solution. Away from the discontinuous step, all three methods give almost same results, the reflected shock wave are all captured. While at the adjacent of discontinuity, the result made by modified HR is different from the others, the under estimation is clear to see at the left cell of the discontinuity compared with the reference solution. The jump of the bottom become smaller, the under estimation become weaker. And when the jump become small enough, the under estimation will disappear. So the result made HR and new HR method are more believable for this case.

5.6 Malpasset dam-break event

As a real-life application, we apply the proposed scheme to the Malpasset dam-break, which is one of the benchmark cases recommended by the EU CADAM project [Morris, 2000]. The Malpasset dam was located in the Reyran River valley in France, about 12 km upstream of Frejus in southern France. After the dam broke, the maximum water depths of the flood wave were identified at 17 points along the banks of the valley based on the trace marks left by flood inundation, and the arrival times were also determined at 3 electronic transformers [A, B, C]. Additionally, the maximum water depths were measured at 9 gauge points in a physical model of 1:400 scale built by Électricité de France in 1964.

The elevation of the model domain ranges from 20 to 100m above sea level. The initial water levels in the Mediterranean Sea, the reservoir and its dam are 0m, 100m and 56.8m, respectively. The channel bottom downstream from the dam is assumed to be initially dry. The solid wall condition is imposed along boundaries everywhere [Zhou et al., 2013]. As advised by the previous studies [Brufau et al., 2004,Audusse and Bristeau, 2005,Zhou et al., 2013] a uniform Manning coefficient of 0.033 s/m$^{1/3}$ was specified across the simulation domain.

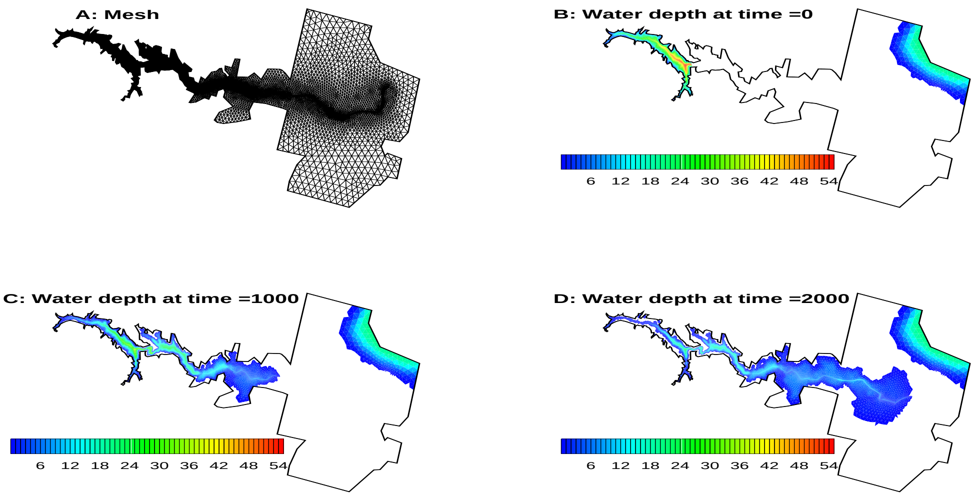

Figure 11: Malpasset dambreak problem using the new HR scheme: Simulation mesh with 2600 elements and 13541 points; Water depth at times 0s, 1000s and 2000s.

The physical domain and the mesh, including 2600 elements and 13541 points are shown in subfigure A of Figure 11. We used the three HR schemes proposed in the paper for the simulation. Since the differences between these schemes are very small and invisible in the plots, we only show the water depth computed by the new HR scheme. In sub-figures B, C, and D of Figure 11, we display the solution at times 0s, 1000s and 2000s. All result are acceptable and agree with those in [Brufau et al., 2004, Audusse and Bristeau, 2005, Zhou et al., 2013]. To gain further insight, we also show maximum water levels at 17 police survey points (see Table 1) and 9 gauge points (see Table 2). While the root mean square difference (RMSD) between any of the schemes and the 17 measurements is between 3.0 and 3.1, the analogous differences between the three schemes are 0.139 (HR-MOR), 0.060 (HR-CN), and 0.117 (MOR-CN). Similarly, at the 9 gauge points the differences between the measurements and the HR schemes are almost 4, and the difference between the schemes are only 0.046 (HR-MOR), 0.038 (HR-CN), and 0.040 (MOR-CN). The arrival times at the three electric transformers are shown in table 3, all result are acceptable and comparable because there is not big abrupt discontinuity of the bottom. Actually all of these numerical arrival times are delayed similar with that shown in example 5.4, and the modified and new HR methods can still give a little bit higher resolution. These results suggest that the modelling errors between the three HR schemes are far below the modelling error between the shallow water equations and the real event.

Table 1: Maximum water levels at 17 police survey points and root mean square error between measurements and the three HR schemes.

Points	x	y	Measurements	HR	Modified HR	New HR
1	4913.11	4244.01	79.15	76.93	76.97	76.95
2	5159.75	4369.62	87.20	88.18	88.21	88.16
3	5790.63	4177.76	54.90	55.40	55.31	55.33
4	5886.54	4503.97	64.70	58.75	58.48	58.56
5	6763.05	3429.60	51.10	46.59	46.10	46.57
6	6929.97	3591.87	43.75	44.06	44.05	44.03
7	7326.02	2948.78	44.35	41.22	41.22	41.22
8	7441.01	3232.12	38.60	33.77	33.71	33.64
9	8735.94	3264.61	31.90	33.20	33.24	33.20
10	8628.60	3604.63	40.75	38.73	38.74	38.71
11	9761.13	3480.36	24.15	24.65	24.66	24.65
12	9800.00	2414.79	24.90	25.91	25.92	25.91
13	10957.00	2651.94	17.25	23.70	23.70	23.70
14	11156.99	3800.72	20.70	20.69	20.69	20.69
15	11689.05	2592.36	18.60	19.10	19.12	19.10
16	11626.05	3406.80	17.25	19.82	19.82	19.82
17	12333.72	2269.74	14.00	15.62	15.62	15.62
RMSD	-	-	-	3.00	3.08	3.04

6 Conclusions

We have introduced a new hydrostatic reconstruction scheme for the shallow water equations. In singular layers, where both the conservative variables and the bottom topography are discontinuous, the non-conservative product of measures is separated according to a

Table 2: Maximum water level at 9 gauge points and root mean square error between measurements and the three HR schemes.

points	x	y	Measure-ments	HR	Modified HR	New HR
6	4947.46	4289.71	84.20	81.36	81.39	81.30
7	5717.30	4407.61	49.10	56.36	56.24	56.27
8	6775.14	3869.23	54.00	53.81	53.83	53.80
9	7128.20	3162.00	40.20	48.49	48.51	48.48
10	8585.30	3443.08	34.90	37.29	37.31	37.26
11	9674.97	3085.89	27.40	25.79	25.80	25.79
12	10939.15	3044.78	21.50	19.47	19.48	19.47
13	11724.37	2810.41	16.10	17.81	17.84	17.81
14	12723.70	2485.08	12.90	12.95	12.96	12.95
RMSD	-	-	-	4.01	3.99	3.99

Table 3: Flood arrival times at three electric transformers.

trans-formers	x	y	Measure-ments	HR	Modified HR	New HR
A	5550	4400	100	124	128	125
B	11900	3250	1240	1317	1310	1313
C	13000	2700	1420	1431	1423	1425

natural definition of the bottom topography in the presence of an embedded wet-dry front. An intermediate water height is defined to the left and the right of the front, and the source term can then be evaluated. This construction only affects a few lines of code of the original hydrostatic reconstruction scheme [Audusse et al., 2004]. The construction via singular layers simplifies and clarifies the derivation of the classical HR schemes, and it can be used to design future schemes.

We have proved positivity of the water height, well-balancing of the lake at rest, and a semi-discrete entropy inequality for our scheme. For a number of challenging downhill flows studied recently in the literature, the new scheme yields superior results.

Acknowledgment. The research of G. Chen and S. Noelle are supported by DFG Grant NO361/3-1 and No361/3-2. G. Chen is partially supported by the National Natural Science Foundation of China (No. 11001211, 11371023).

References

[Abgrall and Karni, 2010] Abgrall, R. and Karni, S. (2010). A comment on the computation of non-conservative products. *J. Comput. Phys.*, 229(8):2759–2763.

[Audusse et al., 2004] Audusse, E., Bouchut, F., Bristeau, M.-O., Klein, R., and Perthame, B. (2004). A fast and stable well-balanced scheme with hydrostatic reconstruction for shallow water flows. *SIAM Journal on Scientific Computing*, 25:2050–2065.

[Audusse and Bristeau, 2005] Audusse, E. and Bristeau, M.-O. (2005). A well-balanced positivity preserving "second-order" scheme for shallow water flows on unstructured meshes. *Journal of Computational Physics*, 206(1):311–333.

[Bollermann et al., 2013] Bollermann, A., Chen, G., Kurganov, A., and Noelle, S. (2013). A well-balanced reconstruction of wet/dry fronts for the shallow water equations. *Journal of Scientific Computing*, 56(2):267–290.

[Bouchut, 2004] Bouchut, F. (2004). *Nonlinear stability of finite volume methods for hyperbolic conservation laws and well-balanced schemes for sources*. Frontiers in Mathematics. Birkhäuser Verlag, Basel.

[Brufau et al., 2004] Brufau, P., García-Navarro, P., and Vázquez-Cendón, M. (2004). Zero mass error using unsteady wetting–drying conditions in shallow flows over dry irregular topography. *International Journal for Numerical Methods in Fluids*, 45(10):1047–1082.

[Castro et al., 2006] Castro, M., Gallardo, J. M., and Parés, C. (2006). High order finite volume schemes based on reconstruction of states for solving hyperbolic systems with nonconservative products. Applications to shallow-water systems. *Math. Comp.*, 75(255):1103–1134.

[Castro et al., 2008] Castro, M. J., LeFloch, P. G., Muñoz-Ruiz, M. L., and Parés, C. (2008). Why many theories of shock waves are necessary: Convergence error in formally path-consistent schemes. *Journal of Computational Physics*, 227(17):8107–8129.

[Dal Maso et al., 1995] Dal Maso, G., Lefloch, P. G., and Murat, F. (1995). Definition and weak stability of nonconservative products. *J. Math. Pures Appl. (9)*, 74(6):483–548.

[Delestre et al., 2012] Delestre, O., Cordier, S., Darboux, F., and James, F. (2012). A limitation of the hydrostatic reconstruction technique for shallow water equations. *Comptes Rendus Mathematique*, 350(13-14):677–681.

[Godlewski and Raviart, 1996] Godlewski, E. and Raviart, P.-A. (1996). *Numerical Approximation of Hyperbolic Systems of Conservation Laws*, volume 118 of *Applied Mathematical Sciences*. Springer Verlag.

[Harten et al., 1983] Harten, A., Lax, P. D., and Leer, B. v. (1983). On upstream differencing and godunov-type schemes for hyperbolic conservation laws. *SIAM Review*, 25(1):35–61.

[Kurganov and Levy, 2002] Kurganov, A. and Levy, D. (2002). Central-upwind schemes for the Saint-Venant system. *ESAIM: Mathematical Modelling and Numerical Analysis*, 36:397–425.

[Lax and Wendroff, 1960] Lax, P. and Wendroff, B. (1960). Systems of conservation laws. *Comm. Pure Appl. Math.*, 13:217–237.

[Morales de Luna et al., 2013] Morales de Luna, T., Castro Díaz, M. J., and Parés, C. (2013). Reliability of first order numerical schemes for solving shallow water system over abrupt topography. *Applied Mathematics and Computation*, 219(17):9012–9032.

[Morris, 2000] Morris, M. (2000). CADAM: Concerted action on dambreak modeling–final report. *Rep. No. SR*, 571.

[Muñoz-Ruiz and Parés, 2011] Muñoz-Ruiz, M. L. and Parés, C. (2011). On the convergence and well-balanced property of path-conservative numerical schemes for systems of balance laws. *J. Sci. Comput.*, 48(1-3):274–295.

[Noelle et al., 2007] Noelle, S., Xing, Y., and Shu, C.-W. (2007). High-order well-balanced finite volume WENO schemes for shallow water equation with moving water. *Journal of Computational Physics*, 226(1):29–58.

[Noelle et al., 2009] Noelle, S., Xing, Y., and Shu, C.-W. (2009). High-order well-balanced schemes. *Numerical Methods for Relaxation Systems and Balance Equations. Italy: Quaderni di Matematica, Dipartimento di Matematica, Seconda Universita di Napoli.*

[Parés, 2006] Parés, C. (2006). Numerical methods for nonconservative hyperbolic systems: a theoretical framework. *SIAM J. Numer. Anal.*, 44(1):300–321.

[Roe, 1981] Roe, P. L. (1981). Approximate riemann solvers, parameter vectors, and difference schemes. *Journal of Computational Physics*, 43:357–372.

[Rusanov, 1961] Rusanov, V. V. (1961). The calculation of the interaction of non-stationary shock waves with barriers. *Ž. Vyčisl. Mat. i Mat. Fiz.*, 1:267–279.

[Toro, 1999] Toro, E. F. (1999). *Riemann Solvers and Numerical Methods for Fluid Dynamics.* Springer.

[Zhou et al., 2013] Zhou, F., Chen, G., Huang, Y., Yang, J. Z., and Feng, H. (2013). An adaptive moving finite volume scheme for modeling flood inundation over dry and complex topography. *Water Resources Research*, 49:1914–1928.

[Zhou et al., 2001] Zhou, J. G., Causon, D. M., Mingham, C. G., and Ingram, D. M. (2001). The surface gradient method for the treatment of source terms in the shallow-water equations. *Journal of Computational Physics*, 168(1):1–25.